Social Networks 82 (2025) 111–133

Contents lists available at ScienceDirect

Social Networks

journal homepage: www.elsevier.com/locate/socnet

An Optimal Transport approach to model the community structure of the International Trade Network

Rossana Mastrandrea [a], Paolo Pagnottoni [b], Nicolò Pecora [c], Alessandro Spelta [d,*]

[a] IMT School for Advanced Studies, Piazza S. Francesco 19, Lucca, 55100, Italy
[b] Department of Economics, University of Insubria, Via Monte Generoso 71, Varese, 21100, Italy
[c] Department of Economics and Social Sciences, Catholic University, Via E. Parmense 84, 29122, Piacenza, Italy
[d] Department of Economics and Management, University of Pavia, Via S. Felice 5, Pavia, 27100, Italy

ARTICLE INFO

JEL classification:
F14
C65
L14

Keywords:
International Trade Network
Optimal Transport
Modularity
Gravity model

ABSTRACT

This paper introduces a novel framework to analyze the community structure of the International Trade Network by integrating Optimal Transport theory with a gravity-based null model. Unlike traditional modularity approaches, our method accounts for socio-economic constraints and assesses the extent to which residual heterogeneity shapes the community structure. This allows for a more economically grounded and policy-relevant analysis, enabling scenario simulations of economic shocks, trade disruptions, and policy changes. Empirical results show that while our approach aligns with standard modularity methods in stable periods, it outperforms them during crises, capturing deeper economic and financial dynamics. Notably, our findings reveal that the degree of financial development of countries plays a critical role in shaping the emerging partitions.

1. Introduction

In recent decades, international trade relationships have been extensively studied through network theory (Serrano et al., 2007; Garlaschelli et al., 2007; Fagiolo et al., 2008; Bhattacharya et al., 2008; De Benedictis and Tajoli, 2011; Tajoli et al., 2021). The intricate architecture of trade connections (*edges*) exemplifies a complex system where linkages, arising from exchanged goods and services, serve as primary channels of interaction between nations (*nodes*), transmitting economic shocks directly (Squartini and Garlaschelli, 2015; Saracco et al., 2016) and propagating financial ones indirectly (Kali and Reyes, 2010; Schiavo et al., 2010).

Early research on import–export relationships employed a binary representation of the International Trade Network (ITN) (Serrano and Boguñá, 2003; Garlaschelli and Loffredo, 2004a,b; Kali and Reyes, 2007), considering only the presence or absence of links based on trade flow thresholds. Subsequent studies shifted to weighted network representations (Bhattacharya et al., 2008; Fagiolo, 2010; Fronczak and Fronczak, 2012; De Benedictis and Tajoli, 2011), where bilateral links are weighted by the deflated value of trade (imports/exports) over a specific time interval. This shift allowed for accounting for the heterogeneity of trade linkages, offering new insights into structural organization and the roles of countries. Relatedly, Mastrandrea et al. (2014) proposed the "irreducibility conjecture", highlighting the distinct *functional roles* of node degree and strength in shaping network structure.

Topological measures, such as scale-free or small-world properties, centrality measures and motifs are often used to characterize the structural organization of the weighted ITN. Of particular interest is the identification of *communities*, or groups of nodes with more segregation than integration, which represent mesoscale structures distinct from individual nodes and the overall network (Girvan and Newman, 2002; Newman, 2004; Rosvall and Bergstrom, 2008; Porter et al., 2009; Aldecoa and Marin, 2011; Yang et al., 2013; Malliaros and Vazirgiannis, 2013; Fortunato and Hric, 2016; Jin et al., 2021). The analysis of community structure within the ITN has revealed key insights into global economic integration, including the contrasting effects of globalization, hierarchization, and localization on the mesoscale structure of the network (Barigozzi et al., 2011; Piccardi and Tajoli, 2012; Fan et al., 2014; Zhu et al., 2014; García-Pérez et al., 2016; Cho et al., 2023). For instance, Barigozzi et al. (2011) found that ITN communities closely align with geographical distances, suggesting geography plays a more significant role than political factors in shaping trade patterns. Piccardi and Tajoli (2012) showed that increasing globalization and complexity make mesoscale structures harder to identify. Fan et al.

* Corresponding author.
E-mail addresses: rossana.mastrandrea@imtlucca.it (R. Mastrandrea), paolo.pagnottoni@uninsubria.it (P. Pagnottoni), nicolo.pecora@unicatt.it (N. Pecora), alessandro.spelta@unipv.it (A. Spelta).

https://doi.org/10.1016/j.socnet.2025.03.008
Received 12 June 2024; Received in revised form 24 March 2025; Accepted 24 March 2025
Available online 10 April 2025

(2014) demonstrated that ITN partitions naturally divide countries into three groups, reflecting the core–periphery structure of the network. Additionally, García-Pérez et al. (2016) revealed growing heterogeneity in trade distances and noted that preferential trade agreements often fail to align with trade communities or reduce internal trade barriers.

In this context, modularity maximization plays a crucial role in community detection (Newman, 2006; Brandes et al., 2007; Fortunato, 2010; Good et al., 2010; Chen et al., 2014), as it identifies the optimal partition of a system by maximizing its deviation from a benchmark model in terms of within-group connectivity. The benchmark model is designed to preserve specific local features of the real network, referred to as *constraints*, while remaining random otherwise. Modularity-based community detection thus seeks to identify groups of nodes with high intra-cluster connectivity and low inter-cluster connectivity. In the ITN, community analysis aims to reveal clusters of countries with privileged trade relationships driven by factors such as geographical proximity, shared language or religion, historical ties, and preferential trade agreements. However, communities identified through modularity maximization may be significantly shaped by economic factors affecting trade flows. While this approach offers valuable insights, it may fail to fully capture the underlying mechanisms that structure the network. For example, standard modularity maximization might overlook key structural features or interactions that, while not directly economic in nature, are nonetheless essential to the overall functioning of the network.

In this paper, we propose a modification of the standard modularity function proposed by Newman and Girvan (2004), henceforth the NG modularity, to cope with this issue. Specifically, we introduce a novel null model within the modularity function, including major economic constraints which are well-known for playing a fundamental role in the formation of trade linkages. In particular, our model integrates insights from the gravity approach, particularly accounting for countries' size, distances, and additional socio-economic features. Indeed, the extensive empirical literature on gravity models (Anderson, 1979; Bergstrand, 1985; Leamer and Levinsohn, 1995; Evenett and Keller, 2002; Overman et al., 2003; Fagiolo, 2010; De Benedictis and Taglioni, 2011; Duenas and Fagiolo, 2013; Chaney, 2018) underscores the effectiveness of this multiplicative model, inspired by the physical gravity equation, to largely explain the international trade flows. Incorporating gravity-based constraints is essential, as they offer a more realistic portrayal of the complex interplay between influencing factors, providing a nuanced understanding of network dynamics.

Against this background, we develop a null model based on gravity equations and Optimal Transport (OT) theory (see Villani, 2009; Chen et al., 2021; Petersen et al., 2021; De Giuli and Spelta, 2023; Spelta and Pecora, 2024) that serves as a benchmark in the modularity function. We call this approach the *OT-gravity* method. OT assesses the minimal effort required to redistribute probability mass from an input distribution to match a target distribution, considering the cost associated with mass transportation. We leverage this principle to refine the modularity function, embedding economic information into the community detection process. The proposed OT-gravity framework extends beyond traditional topological analysis by incorporating key trade determinants, such as Gross Domestic Product (GDP), geographic distance, and trade agreements. This integration ensures that network analysis aligns with empirical economic behavior, while the resulting constraints offer a theoretical basis for examining the mesoscale structure of the ITN. In other words, unlike traditional modularity approaches, our method explicitly accounts for socio-economic constraints and evaluates the extent to which residual heterogeneity beyond such constraints influences community structure. A significant advancement over conventional network analysis methods lies in the framework's economic realism when identifying community structures. The OT-gravity framework ensures that identified network partitions reflect both connectivity patterns and underlying socioeconomic drivers of trade interactions. This theoretical setting enables analysis of shock propagation through network communities, enhancing the framework's utility for policy applications. The methodology facilitates the simulation of various scenarios, including trade disruptions and GDP fluctuations, to evaluate their impact on ITN community structure. Moreover, model calibration using empirical data ensures accurate reproduction of observed trade flows under baseline conditions. Deviations in simulated outcomes under modified constraints provide quantitative insights into community resilience and adaptability.

Our work also engages with the spatial network literature. As a matter of fact, the ITN is an example of complex systems organized in the form of a network embedded in space (Expert et al., 2011). When considering networks where nodes occupy positions in a determined space, spatial constraints may have a strong effect on their connectivity patterns (see e.g. Butts, 2003; Butts and Acton, 2011; Butts, 2012; Daraganova et al., 2012; Preciado et al., 2012; Almquist and Butts, 2015). In particular, Butts and Acton (2011), Butts et al. (2012) provide critical insights into spatial variability and modeling. These studies underline the importance of accounting for localized interactions, spatial heterogeneity, and non-spatial factors in shaping network connectivity. Our OT-gravity modularity framework aligns with these principles by incorporating gravity-based constraints and using OT theory to establish joint distributions, allowing for the construction of flexible and data-driven null models. This integration ensures that the OT-gravity modularity framework considers key spatial and economic dimensions, offering a comprehensive perspective on the mesoscale structure of empirical networks such as the ITN. While (Butts et al., 2012) highlight the role of geographical variability resulting in non-homogeneous patterns of connectivity, our OT-gravity framework captures this variability in an indirect way through gravity model constraints, such as distance, trade agreements, and contiguity. By doing so, our approach not only aligns with spatial modeling principles but also provides a novel methodology for evaluating community structures influenced by both spatial and economic factors.

Results from the gravity model estimation show that the key variables found to play a significant role in modeling bilateral trade in the extant literature are confirmed (Fagiolo, 2010; Duenas and Fagiolo, 2013). The GDP of the destination and source countries, trade agreements, shared borders, and common language exhibit positive association with bilateral trade flows, while factors such as the distance between countries and the likelihood of being landlocked show a negative association. An exploratory analysis of fitted values reveals that trade flows predictions remain stable, irrespective of whether fixed effects are included in the model specification, providing a robust foundation for the modularity null model and supporting the robustness of the conclusions drawn from the OT-gravity approach. Incorporating gravity estimates in the modularity function provides modularity values which are consistently larger than those yielded by standard null models, thus reflecting a better partition quality. Furthermore, differently from the NG modularity, our proposal yields a smaller number of communities, where a minority of communities predominantly houses the majority of nodes. Specifically, the partitions derived from the OT-gravity modularity align with the outcomes of the NG modularity during normal business phases, while they exhibit significant differences during crisis periods such as the Great Financial Crisis and the COVID-19 outbreak.

We then explore to which extent the community structure of the ITN, obtained via the OT-gravity modularity, can be explained by residual sources of variation, other than the socio-economic ones, thus identifying *extra* drivers behind the emerging partitions. In particular, we leverage machine learning classifiers to evaluate whether the financial development of a country is a good discriminant when considering the emerging communities derived from the OT-gravity modularity. In other words, by building on the link existing between financial development and international trade (Beck, 2002; Leibovici, 2021), we expect these covariates to show higher variations across partitions obtained through the OT-gravity method compared to the NG modularity, thereby providing more accurate predictions. We find that financial development indices do generally contribute to explain the emerging community structure of the ITN after having controlled for socio-economic variables, especially during crisis phases.

Ultimately, in contrast to the conventional modularity framework, our approach allows to conduct scenario analysis by incorporating functional relationships which elucidate interactions among variables. We therefore conduct a policy experiment in which we evaluate changes in the community structure of the ITN network following a global shock to the economy. Specifically, we model two scenarios related to the COVID-19 pandemic: one depicting a recovery and another depicting an extended crisis resulting from a negative GDP shock affecting either the G7 or the BRICS economies. The results of the simulated experiments show a rise in the number of communities, with countries forming new clusters based on geographical proximity and historically relevant trade relationships.

Our contribution to the literature features two main aspects. From a methodological viewpoint, we propose a novel approach based on OT theory to construct null models incorporating trade relationships estimated through gravity equations, integrating socio-economic constraints. From an empirical viewpoint, we show how partitions obtained through the OT-gravity modularity can be explained by the financial development of countries. Further, we demonstrate how our proposed method can be employed to conduct scenario analysis assessing the impact of shocks on the ITN community structure.

The remainder of the paper proceeds as follows. Section 2 introduces the proposed methodology. Section 3 describes the ITN network data used in the study together with preliminary network statistics. Section 4 illustrates the results of the empirical application, including estimation, community detection, the explanation of community structures through financial indicators, and evidence from the policy experiment. Section 5 concludes and presents future research perspectives.

2. Methodology

In this section, we present our proposal which consists of a tailored modularity function. The proposed modularity offers a nuanced approach to identify and investigate the mesoscale structure of the ITN, acknowledging influences that extend beyond the conventional realms of economic analysis (Expert et al., 2011).

2.1. The International Trade Network (ITN)

We represent the ITN as a graph $G = (V, E)$, where V is the set of countries (nodes) with size $|V| = N$ and E is the set of all connections among them (edges) with size $|E| = L$. Links are then weighted by cross-border trade flows between countries. The resulting network is a directed graph, where a link e is oriented and weighted, connecting a source node i (exporter) with a destination node j (importer). The graph G is then represented by the binary, $A \equiv (a_{i,j})_{1\le i,j\le N}$, and weighted, $W \equiv (w_{i,j})_{1\le i,j\le N}$, adjacency matrices, where $a_{i,j} = 1 (a_{i,j} = 0)$ indicates the presence (absence) of an edge between nodes i and j, while w_{ij} represents the corresponding link weight, namely the amount of goods and services traded from country i to country j. It is worth noticing that, generally, $a_{i,j} \neq a_{j,i}$ as the network is directed and $w_{i,j} \neq w_{j,i}$. Moreover, we define the node out- and in-strength as follows. The out-strength of node i is defined as $s_i^{out} = \sum_j w_{i,j}$, while the in-strength of j is computed as $s_j^{in} = \sum_i w_{i,j}$, representing the total amount of exports and imports of country i and j, respectively. The total amount of exchanged goods and services in the system is given by $w_{tot} = \sum_{i,j} w_{i,j} = \sum_i s_i^{out} = \sum_j s_j^{in}$.

2.2. Modularity maximization

The modularity maximization approach (Newman, 2004, 2006) does not require to fix the number of desired clusters *a priori*. Indeed, it endeavors to autonomously unveil the mesoscale structure inherent in the network, grounding on two main hypothesis: (i) connections within communities are more likely than between them, and (ii) randomly wired networks lack an intrinsic community structure. Therefore, modularity maximization quantifies the extent to which communities are internally connected compared to what would be expected in a random network sharing some properties with the observed one.

Formally, modularity reads as:

$$Q = \frac{1}{L} \sum_{i,j\in V} \left(a_{i,j} - p_{i,j}\right) \delta(c_i, c_j), \tag{1}$$

where V is the set of all nodes in the network, $a_{i,j}$ is the (i, j)th element of the adjacency matrix associated to it and L is the total number of links in the network. $\delta(c_i, c_j)$ stands for the Kronecker delta equal to 1 if nodes i and j belong to the same community ($c_i \equiv c_j$), or zero otherwise. In this formulation, $p_{i,j}$ introduces the aforementioned *randomness* as it represents the probability to observe a link between nodes i and j given some specific attributes, i.e. *constraints*. These constraints are associated with well-known, and generally local, information regarding the organization of the network, encompassing factors such as the total number of links and nodes, degree and strength. Such objects are essential as they represent the only information of the real network preserved in the construction of the benchmark null model.

In a weighted network framework, the most standard choice for the reference null model is:

$$p_{i,j} = \frac{s_i^{in} s_j^{out}}{w_{tot}}, \tag{2}$$

and, accordingly, the modularity function reads as:

$$Q = \frac{1}{w_{tot}} \sum_{i,j\in V} \left(w_{i,j} - p_{i,j}\right) \delta(c_i, c_j). \tag{3}$$

This approach assumes that the connectivity patterns in the network are primarily influenced by the nodes' relative strengths, emphasizing the significance of this weighted attribute in shaping the overall network topology. The idea of focusing on node strengths aligns with the assumption that the network is well-mixed, implying that any node has the potential to connect with any other node simply given its total outgoing and in-going trade flows. The traditional null models included in the modularity function depend exclusively on topological properties of the system (binary or weighted), neglecting exogenous variables, if any, but implicitly assuming their effect in shaping the actual observed network of interactions. However, in economic networks such as the ITN, the gravity model has proved a highly rate of success in estimating and explaining trade flows among countries. Thus, it appears a natural choice to include it in the benchmark model. Incorporating gravity-inspired constraints becomes crucial, as they might better capture a more realistic representation of the complex interplay between the various influencing factors, allowing to wash away their effect while studying the network mesoscale organization.

2.3. Gravity model

The most general formulation of the gravity model (Silva and Tenreyro, 2006) reads as:

$$\begin{aligned} w_{i,j} =& \alpha_0 \left[\mathrm{GDP}_i^{\alpha_1} \mathrm{GDP}_j^{\alpha_2} \mathrm{DIST}_{i,j}^{\alpha_3}\right] \cdot \left[\prod_{k=1}^{K} X_{i,k}^{\beta_{1,k}} X_{j,k}^{\beta_{2,k}}\right] \\ & \cdot \exp\left\{\sum_{h=1}^{H} \varphi_h D_{i,j,h} + \sum_{l=1}^{L} (\theta_{1,l} Z_{i,l} + \theta_{2,l} Z_{j,l}) + (\zeta_i C_i + \zeta_j C_j)\right\} \eta_{i,j} \end{aligned} \tag{4}$$

where $w_{i,j}, i, j = 1, \dots, N$ is the $N(N-1)$-dimensional vector of bilateral trade flows while $(\alpha, \beta, \varphi, \theta, \zeta)$ are unknown vectors of parameters to be estimated. The variable GDP represents country gross-domestic product, $DIST$ is the geodesic geographical distance between two countries, determined as the Haversine distance. X_i are vectors of country-specific variables (other than GDP), Z_i are vectors of country-specific dummy variables, $D_{i,j,h}$ are vectors of edge-specific dummy variables (different from distance), C_i represent country-specific fixed effects and $\eta_{i,j}$ is a normally distributed error term which is independent on the regressors.

Following Fagiolo (2010) and Duenas and Fagiolo (2013), the model in Eq. (4) simplifies into:

$$\begin{aligned} w_{i,j} = \log \Big(\alpha_0 & \left[\mathrm{GDP}_i^{\alpha_1} \mathrm{GDP}_j^{\alpha_2} \mathrm{DIST}_{i,j}^{\alpha_3}\right] \cdot \left[\mathrm{AREA}_i^{\beta_1} \mathrm{AREA}_j^{\beta_2} \mathrm{POP}_i^{\beta_3} \mathrm{POP}_j^{\beta_4}\right] \\ & \cdot \exp\{\theta_1 \mathrm{CTG}_{i,j} + \theta_2 \mathrm{COML}_{i,j} + \theta_3 \mathrm{COL}_{i,j} + \theta_4 \mathrm{TA}_{i,j} + \theta_5 \mathrm{COMC}_{i,j} \\ & + \phi_1 \mathrm{LL}_i + \phi_2 \mathrm{LL}_j\} \eta_{i,j} \Big), \end{aligned} \tag{5}$$

where $(\alpha, \beta, \theta, \phi)$ are the vectors of coefficients to be estimated. The variables $AREA$ and POP stand for the area (in km^2) of a country and its population, respectively. CTG is a contiguity dummy equal to 1 if two countries share a common border while $COML$ is a dummy equal to 1 if the official language (or mother tongue or second language) of the two countries is the same. The variable COL is a dummy equal to 1 if the two countries share a substantial colonizer-colonized relationship. TA represents the trade agreement dummy between two countries and it is 1 if both countries are involved in a preferential trade agreement, while $COMC$ is a dummy equal to 1 if both countries share the same currency. Finally, LL is a country dummy variable equal to 1 for landlocked countries. Instead, $\eta_{i,j}$ represents the normally distributed error term.

Estimating Eq. (5) poses several challenges, encompassing the treatment of zero-valued flows (Silva and Tenreyro, 2006; Linders and De Groot, 2006; Burger et al., 2009), non-linearity, and heteroscedasticity (Silva and Tenreyro, 2006), as well as addressing issues of endogeneity and omitted-term biases (Baldwin and Taglioni, 2006). To concurrently address these problems, we employ a zero-inflated Poisson (ZIP) pseudo-maximum likelihood (PPML) model for the estimation of Eq. (5), as proposed by Burger et al. (2009). The zero-inflated model reads as:

$$Q(\mathrm{W}) = \prod_{i \neq j} q_{i,j}(w_{i,j}) = \prod_{i \neq j} r_{i,j}^{a_{i,j}} (1 - r_{i,j})^{1 - a_{i,j}} \cdot q_{i,j}(w_{i,j} | a_{i,j}) = R(\mathrm{A}) Q(\mathrm{W}|\mathrm{A}), \tag{6}$$

and indicates that the probability of observing links reported in the weighted adjacency matrix W can be obtained as the product of the probability $R(A)$ of observing the binary adjacency matrix A and the conditional probability $Q(W|A)$. The zero-inflated Poisson is defined by the elements:

$$r_{i,j}^{\mathrm{ZIP}} = \frac{G_{i,j}}{1 + G_{i,j}} (1 - e^{-z_{i,j}}) \tag{7}$$

$$q_{i,j}^{\mathrm{ZIP}} \left(w_{i,j} \mid a_{i,j} = 1\right) = \begin{cases} \frac{z_{i,j}^{w_{i,j}} e^{-z_{i,j}}}{(1 - e^{-z_{i,j}}) w_{i,j}!}, & w_{i,j} > 0 \\ 0, & w_{i,j} \leqslant 0 \end{cases} \tag{8}$$

The ZIP model can then be estimated by maximizing the likelihood:

$$\begin{aligned} \mathcal{L}_{\mathrm{ZIP}} = \sum_{i \neq j} \Big[& a_{i,j} \ln G_{i,j} - a_{i,j} \ln\left(1 + G_{i,j} e^{-z_{i,j}}\right) \\ & + \ln\left(1 + G_{i,j} e^{-z_{i,j}}\right) - \ln\left(1 + G_{i,j}\right) \\ & + w_{i,j} \ln z_{i,j} - a_{i,j} z_{i,j} - a_{i,j} \ln \Gamma\left[w_{i,j} + 1\right] \Big], \end{aligned} \tag{9}$$

where both G and z are defined by the r.h.s. of Eq. (5). The estimated model furnishes a graph sharing the same binary topology of the observed one and fully characterized by the estimated weight matrix $\hat{W} = \{\hat{w}_{i,j}\}$.

2.4. Fixed effects gravity model

The model described in Eq. (5) draws on the gravity framework outlined by Fagiolo (2010) and Duenas and Fagiolo (2013). This framework relates bilateral trade flows $(w_{i,j})$ to the economic size of trading partners, geographical and demographic factors, and various trade-related dummy variables. The above model can be interpreted as a reduced-form gravity model where the coefficients of GDP, distance, and other covariates capture their direct effects on trade.

However, this specification does not fully address unobserved heterogeneity at the country level, such as institutional quality, trade policies, or unmeasured geographic characteristics, which may bias empirical estimates. To address these issues, we reformulate the gravity model using exporter and importer fixed effects. Fixed effects absorb the unobserved, country-specific factors that influence trade. In the fixed effects specification, the terms GDP, AREA, and POP, along with any other variables that are constant for a specific exporter or importer, are absorbed into the fixed effects. Accordingly, the model reads as:

$$\begin{aligned} \ln(w_{i,j}) = \alpha_i + \chi_j + \alpha_3 \ln(\mathrm{DIST}_{i,j}) + \theta_1 \mathrm{CTG}_{i,j} + \theta_2 \mathrm{COML}_{i,j} + \\ \theta_3 \mathrm{COL}_{i,j} + \theta_4 \mathrm{TA}_{i,j} + \theta_5 \mathrm{COMC}_{i,j} + \eta_{i,j}, \end{aligned} \tag{10}$$

where α_i is the exporter fixed effect, capturing all exporter-specific characteristics, χ_j represents the importer fixed effect, capturing all importer-specific characteristics, while $\ln(\mathrm{DIST}_{i,j})$ and the bilateral dummy variables (CTG, COML, COL, TA, COMC) remain unchanged in the model as they vary bilaterally and are not collinear with the fixed effects. The inclusion of fixed effects has two main implications. First, the absorption of country-specific variables is taken into account, which means that such variables are no longer estimated separately because their variation is fully captured by fixed effects α_i and χ_j. Second, the method provides unbiased estimates of bilateral effects, which means that the coefficients on $\mathrm{DIST}_{i,j}$, $\mathrm{CTG}_{i,j}$, and other bilateral dummy variables represent their effects after controlling for all exporter- and importer-specific heterogeneity.

The fixed effects model provides a robust way to address unobserved heterogeneity, ensuring that the estimates of bilateral trade determinants are not biased by omitted country-specific variables (Yotov et al., 2016; Yotov, 2024). This adjustment reflects the transition from a traditional gravity framework to the structural gravity model, as highlighted by Anderson and Van Wincoop (2003). In this way we account for multilateral resistance by including a dummy for each origin and a dummy for each destination, the so-called origin and destination effect (Hummels, 1999).

Notably, Fally (2015) demonstrated that, under reasonable assumptions, the estimated effects inherently satisfy these conditions when the gravity equation is estimated using PPML. Consequently, the multilateral resistance indexes can be directly recovered from the estimated effects. Furthermore, Fally (2015) established that PPML is the only pseudo-maximum likelihood estimator possessing this property. Building on these findings, Anderson et al. (2018) introduced a method for computing the general equilibrium effects of trade policies, leveraging a structural gravity model and the unique properties of the PPML estimator (see also Yotov et al., 2016).

2.4.1. Incorporating the binary network structure into the gravity model

In addition to fixed effects and bilateral dummy variables, the binary network structure of import–export relationships can be explicitly incorporated into the gravity model. This network structure is represented as an adjacency matrix, where each element indicates whether there exists a trade relationship between two countries. The binary structure can be included in the model as an additional regressor, leading to the following model specification:

$$\begin{aligned} \ln(w_{i,j}) = \alpha_i + \chi_j + \alpha_3 \ln(\mathrm{DIST}_{i,j}) + \theta_1 \mathrm{CTG}_{i,j} + \theta_2 \mathrm{COML}_{i,j} + \\ + \theta_3 \mathrm{COL}_{i,j} + \theta_4 \mathrm{TA}_{i,j} + \theta_5 \mathrm{COMC}_{i,j} + \psi a_{i,j} + \eta_{i,j}. \end{aligned} \tag{11}$$

The inclusion of $a_{i,j}$ allows us to capture the presence or absence of a trade relationship as a determinant of trade intensity. The binary network captures the structural dependencies of trade relationships, reflecting how the existence of trade links influences observed trade flows. While fixed effects absorb country-specific factors and bilateral determinants capture cost-related effects, $a_{i,j}$ summarizes the binary structure of the observed trade network, providing a complementary lens to understand trade flows. By incorporating the binary network structure, we are able to capture the structural relationships between countries that other covariates may not fully explain, such as geopolitical or historical ties not directly observed in the data. The estimation proceeds using a PPML estimator, where $a_{i,j}$ is included as a binary variable, ensuring that the presence or absence of trade relationships is accounted for alongside fixed effects and other covariates.

2.5. Panel gravity model with exporter-time, importer-time, and time fixed effects

The use of panel gravity models with exporter-time and importer-time fixed effects, as emphasized by Baldwin and Taglioni (2006), allows to properly address unobserved heterogeneity and dynamic persistence in bilateral trade flows. Moreover, including time fixed effects makes it possible to account for common shocks and global trends affecting trade in each year. These enhancements are crucial for obtaining unbiased and reliable estimates of bilateral trade determinants. We extend our empirical analysis by estimating a panel gravity model that incorporates exporter-time, importer-time, and time fixed effects (see also Larch et al., 2019). This specification allows us to control for all time-varying country-specific factors and global trade shocks, in addition to explicitly model time-invariant bilateral characteristics. The estimated model takes the following form:

$$\begin{aligned}\ln(w_{i,j,t}) = \alpha_{i,t} + \chi_{j,t} + \delta_t + \alpha_3 \ln(\mathrm{DIST}_{i,j}) + \theta_1 \mathrm{CTG}_{i,j,t} + \\ + \theta_2 \mathrm{COML}_{i,j,t} + \theta_3 \mathrm{COL}_{i,j,t} + \theta_4 \mathrm{TA}_{i,j,t} + \theta_5 \mathrm{COMC}_{i,j,t} + \eta_{i,j,t},\end{aligned} \tag{12}$$

where $w_{i,j,t}$ denotes bilateral trade flows between exporter i and importer j in year t. The exporter-time fixed effects ($\alpha_{i,t}$) capture all time-varying characteristics of the exporting country, including GDP changes, trade policy shifts, and multilateral resistance terms. Importer-time fixed effects ($\chi_{j,t}$) absorb all importer-specific time-varying factors, such as demand shocks or changes in import regulations. The inclusion of time fixed effects (δ_t) controls for global phenomena and trade shocks that simultaneously affect all country pairs, such as worldwide recessions, geopolitical events, or global supply chain disruptions.

The bilateral regressors in the model include both static and time-varying factors. While geographical distance ($\ln(\mathrm{DIST}_{i,j})$) is time-invariant, variables such as common trade agreements ($\mathrm{CTG}_{i,j,t}$), common language ($\mathrm{COML}_{i,j,t}$), colonial ties ($\mathrm{COL}_{i,j,t}$), active trade agreements ($\mathrm{TA}_{i,j,t}$), and common currency arrangements ($\mathrm{COMC}_{i,j,t}$) are allowed to vary over time, acknowledging the dynamic nature of international trade relationships. The error term ($\eta_{i,j,t}$) captures all unobserved bilateral shocks and stochastic variations.

This specification improves on the repeated cross-sectional analysis by ensuring that estimated coefficients for time-varying bilateral trade determinants are not confounded by unobserved country-level dynamics or global trends. In particular, the simultaneous inclusion of $\alpha_{i,t}$, $\chi_{j,t}$, and δ_t removes biases arising from omitted time-varying exporter and importer characteristics and common global factors.

2.6. A novel modularity null model based on optimal transport

In this subsection we outline our proposal of a modularity null model based on OT theory specifically tailored to trade networks such as the ITN. We employ OT to compute the joint distribution between the normalized sum of all imports (in-strength) and the normalized sum of the exports (out-strength), while minimizing transportation costs which are function of the estimates derived from the gravity model. In other words, utilizing OT, we aim at finding a mapping between in- and out-strength by estimating the joint distribution between these two marginals, considering the cost associated with moving a unit mass from the in-strength distribution to the out-strength distribution.

We define the in-strength distribution across the N nodes as $\mu := \sum_{i=1}^{N} \mu_i d_i$. Similarly, the out-strength distribution is $\nu := \sum_{i=1}^{N} \nu_i d_i$. The variable d_i represents a generic Dirac measure at i. Such distributions are fully characterized by the probability mass vectors on the simplex Σ, namely $\mu \in \Sigma_N$ and $\nu \in \Sigma_N$, where $\mu_i = s_i^{in} / \sum s^{in}$ and $\nu_i = s_i^{out} / \sum s^{out}$. We can then define the distance between μ and ν as:

$$\mathcal{W}(\mu,\nu) := \min_{P \in \Pi(\mu,\nu)} \sum_{i=1}^{m} \sum_{j=1}^{m} p_{i,j} \xi_{i,j}. \tag{13}$$

The optimal transport plan $P \in \Pi(\mu,\nu)$ determines the coupling between the in- and out strength distributions on the space $\{1,\dots,N\} \times \{1,\dots,N\}$, namely the joint distribution which satisfies the OT principle and defines the null model for the modularity function. The matrix P defines a joint distribution with marginals which coincide with μ and ν. Consequently, P is contained in the transportation polytope $\Pi(\mu,\nu)$ defined as:

$$\Pi(\mu,\nu) := \left\{ P \in \mathbb{R}_+^{N\times N} \mid P \mathbb{1}_N = \mu, P^\top \mathbb{1}_N = \nu \right\}. \tag{14}$$

The cost matrix $\Xi \in \mathbb{R}^{N\times N}$ specifies the transportation cost $\xi_{i,j}$ between country pairs i and j. To incorporate economic information into the modularity function we choose $\xi_{i,j} := 1/\hat{w}_{i,j}$ so to have a high probability of observing a link with high weight between i and j if the estimate $\hat{w}_{i,j}$ derived from the gravity model is high.

In order to determine P, one has to solve a linear assignment problem (LAP) from Eq. (13), whose solution can be obtained via algorithms such as the Hungarian algorithm (Kuhn, 1955) or the Auction algorithm (Bertsekas, 1979), as well as other recent solvers (Rubner et al., 1997; Pele and Werman, 2009). However, these approaches are computationally heavy and slow in practice (Cuturi, 2013). A popular alternative is augmenting the LAP objective in Eq. (13) with an additional entropy regularizer, giving rise to the Sinkhorn operator:

$$\mathcal{W}_\gamma(\Xi,\mu,\nu) := \operatorname*{arg\,min}_{P \in \Pi(\mu,\nu)} \sum_{i=1}^{N} \sum_{j=1}^{N} \left(p_{i,j}, \xi_{i,j} - \gamma E(p_{i,j}) \right), \tag{15}$$

where $\gamma > 0$ is a regularization parameter and $E(p_{i,j}) = -p_{i,j} \log\left(p_{i,j}\right)$ is the entropy, with the convention $0 \log 0 = 0$. The seminal work of Cuturi (2013) showed that the additional entropy regularization term allows for an efficient minimization of Eq. (15). Specifically, this can be obtained via an alternating scheme of Sinkhorn projections. By defining the Gibbs kernel as $K \overset{\text{def.}}{=} e^{-\frac{\Xi}{\gamma}} \in \mathbb{R}_+^{N\times N}$, and a vector $f = \mathbb{1}_N$, one can find P by using the Sinkhorn iterations:

$$g \leftarrow \nu \oslash (Kf) \qquad \text{and} \qquad f \leftarrow \mu \oslash (K^\top g),$$

where $\oslash$ denotes component-wise division. We remark that the parameter γ controls the weight assigned to the cost matrix in the Gibbs kernel. A high value of this parameter implies a uniform Gibbs kernel, thus a less relevant role of the cost matrix and, accordingly, of the gravity model.

As shown by Cuturi (2013), in the limit, this scheme converges to a minimizer of Eq. (15). In practice, we can use a finite number of iterations to achieve a sufficiently small residual. Then the coupling matrix P con be found as:

$$P = \mathrm{diag}(f) K \, \mathrm{diag}(g) \tag{16}$$

and constitutes our OT-gravity null model in the modularity Eq. (3).

To provide an intuition on the null model resulting from our proposal, and the difference with the NG modularity, suppose to observe two countries having a high value of total import and export, respectively. According to the NG null model the interaction between these countries will be high, being the product of the two variables, despite the actual trade flow between them might be low. Differently, in our

Table 1
Descriptive statistics of bilateral trade flows. The table shows the yearly minimum (Min) and maximum (Max) values of trade flows, along with the average ($Mean$), standard deviation (Std), coefficient of variation (Cv), skewness ($Skew$) and kurtosis ($Kurt$).

Year	Min	Max ($\times 10^7$)	Mean ($\times 10^7$)	Std ($\times 10^7$)	Cv	Skew	Kurt ($\times 10^5$)
2000	1.001	2.2495	0.0015	0.0236	10.7531	0.0579	0.0043
2001	1.006	2.1034	0.0014	0.0219	10.5841	0.0569	0.0042
2002	1.001	2.0348	0.0014	0.0216	10.5578	0.0552	0.0040
2003	1.001	2.1796	0.0016	0.0236	10.1339	0.0524	0.0037
2004	1.001	2.5205	0.0019	0.0272	9.9103	0.0514	0.0036
2005	1.001	2.8566	0.0022	0.0310	9.9005	0.0522	0.0036
2006	1.002	2.9969	0.0025	0.0341	9.7946	0.0511	0.0034
2007	1.001	3.1430	0.0029	0.0372	9.3930	0.0487	0.0032
2008	1.005	3.3564	0.0033	0.0405	8.9314	0.0464	0.0029
2009	1.001	2.4656	0.0025	0.0315	9.0530	0.0458	0.0028
2010	1.001	3.1884	0.0031	0.0395	9.3574	0.0473	0.0029
2011	1.002	3.4763	0.0037	0.0450	9.0655	0.0454	0.0027
2012	1.002	3.7843	0.0037	0.0470	9.3000	0.0475	0.0030
2013	1.002	3.9594	0.0037	0.0478	9.4459	0.0488	0.0031
2014	1.003	4.2162	0.0037	0.0493	9.6496	0.0508	0.0034
2015	1.004	4.2954	0.0032	0.0459	10.3412	0.0549	0.0039
2016	1.002	4.0596	0.0031	0.0442	10.1609	0.0532	0.0037
2017	1.004	4.5554	0.0035	0.0483	9.9803	0.0530	0.0037
2018	1.001	5.0093	0.0038	0.0522	9.9243	0.0535	0.0038
2019	1.005	4.2700	0.0037	0.0496	9.6303	0.0501	0.0033
2020	1.001	4.3792	0.0034	0.0467	9.5887	0.0515	0.0036

case, such interaction could be lower if the estimated flow between the two countries is low. This can result from the impact of the covariates included in the gravity model, such as geographical distances, preferential trade agreements or other socio-economic factors.

3. Data description

In this section we provide the description and a preliminary analysis of the data we leverage to empirically test our proposal. We analyze publicly available data on international trade retrieved from different sources. We collect international-trade data taken from the gravity database provided by CEPII.[1] We focus on the period 2000–2020: each observation corresponds to a combination of an exporter country, an importing country, a deflated value of trade flow measured in billions of US dollars and the reference year. The number of countries changes over time, ranging from a minimum value of 179 countries in 2000 to a maximum of 193 countries in 2015.

We first present some relevant summary statistics of the data. To this aim, Table 1 summarizes the main descriptive statistics, clearly highlighting an increasing trend of the maximum and average trade flows over time. This behavior is also associated with a more heterogeneous distribution of such quantities, as suggested by the growing trend of the standard deviation over time. Overall, the coefficient of variation decreases up to the Global Financial Crisis, then increases afterwards until the onset of the trade slow-down of 2015. Moreover, both skewness and kurtosis show a similar dynamics with a minimum reached in correspondence of the Global Financial Crisis, where trade flows among countries have become less skewed to the right and more mesokurtic, being affected by a large negative shock.

From the same database, we also collect data concerning colonial relationships, trade agreements and common language. From the World Bank Development Indicators database, we obtain yearly country-level data for GDP and population.[2] The area in km^2 is retrieved from countrycode database, while landlocked countries information is obtained by the United Nations Geo-scheme.[3,4] We construct distances between country pairs by first collecting polygon data from the Word Bank Official Boundaries and, after having averaged the latitude and longitude coordinates, computing the Haversine distance among points.[5] Data for the common currency dummy is based on the list of currencies provided by the Food and Agriculture Organization of the United Nations and computed following (Fagiolo, 2010).[6] Contiguity data is collected from the Correlates of War Project.[7]

3.1. Preliminary network statistics

To offer a general outlook of the evolution of the ITN, we present some relevant network statistics.[8] We provide an overview of the evolution of the ITN over time in Fig. 1. In particular, we show the snapshot of the ITN related to four specific time points: 2004, 2009, 2014, and 2019. Countries are represented as network nodes, positioned on the map according to their average latitude and longitude coordinates. For sake of readability, we show only the links associated to trade flows higher than the 99th percentile of the flows distribution for each respective time point. Node sizes are proportional to their in-strength centrality, i.e. the sum of all incoming capital flows, emphasizing the roles of the USA, China, and Japan. Node colors correspond to out-strength, i.e. the sum of capital outflows, ranging from blue for lower out-strength values to red for higher ones. Notably, the USA have witnessed a decrease in their out-strength, mirroring a reduction in the value of export flows. China, instead, has shifted from experiencing substantial capital inflows to attaining a notable position characterized by significant capital outflows.

We further compute some basic topological measures, namely: (i) the number of nodes, N, and (ii) links, L, i.e. the total number of trade flow connections in the network; (iii) the fraction between the actual number of crossborder trade flows and the total possible connections, namely the density, shedding light on the network cohesiveness:

$$d = \sum_i \sum_j \frac{a_{i,j}}{N(N-1)}, \tag{17}$$

[1] https://cepii.fr/CEPII/en/bdd_modele/bdd_modele_item.asp?id=8

[2] https://databank.worldbank.org/source/world-development-indicators

[3] https://countrycode.org/

[4] https://en.wikipedia.org/wiki/Landlocked_country

[5] https://datacatalog.worldbank.org/search/dataset/0038272/World-Bank-Official-Boundaries

[6] https://www.fao.org/3/bt976e/bt976e.pdf

[7] correlatesofwar.org

[8] We remind that the topological properties of the ITN and their dynamical evolution have been extensively studied (see e.g. Serrano and Boguñá, 2003; Serrano et al., 2007; Garlaschelli et al., 2007; Fagiolo et al., 2008) and are out of the scope of this paper.

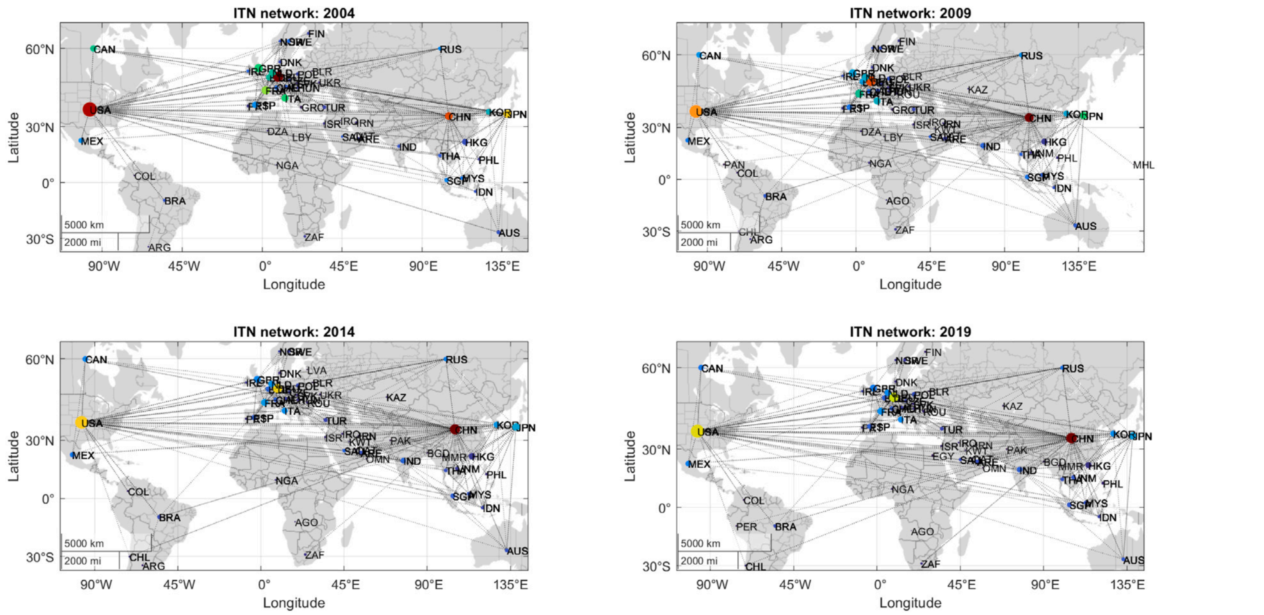

Fig. 1. International Trade Network visualization. The figure shows the geolocalised international trade network in four selected years, namely 2004 (top-left), 2009 (top-right), 2014 (bottom-left), and 2019 (bottom-right). For sake of readability, links represent flows higher than the 99th percentile of the trade distribution in that year. Nodes are located in the centroid of the respective country. The node size is proportional to the in-strength centrality while node colors refer to the out-strength, ranging from blue colors for low values to red colors for high values. (For interpretation of the references to color in this figure legend, the reader is referred to the web version of this article.)

and (iv) the total value of goods traded worldwide:

$$w_{tot} = \sum_i \sum_j w_{i,j}. \tag{18}$$

Fig. 2 illustrates the dynamics of these statistics, showcasing the evolution of the total number of nodes and links along with the total flow and the network density. The top panel shows a surge in both the number of nodes and links until the year 2015, stabilizing afterwards. The bottom panel, instead, presents the behavior of the total flow and network density. The total flow of the ITN exhibits a rapid growth until 2008, followed by a decline due to the Great Financial Crisis and a subsequent recovery. Differently, the density shows a constant growth except for the last two years of the sample. Finally, in order to gain a deeper understanding on how the evolution of crossborder trade agreements influenced the topology of the ITN, we report, in Fig. 3, the survival distributions associated with in- and out-degree and strength. All the panels depict a general upward right shift of the curves, highlighting an increasing hub-like structure of the ITN network.

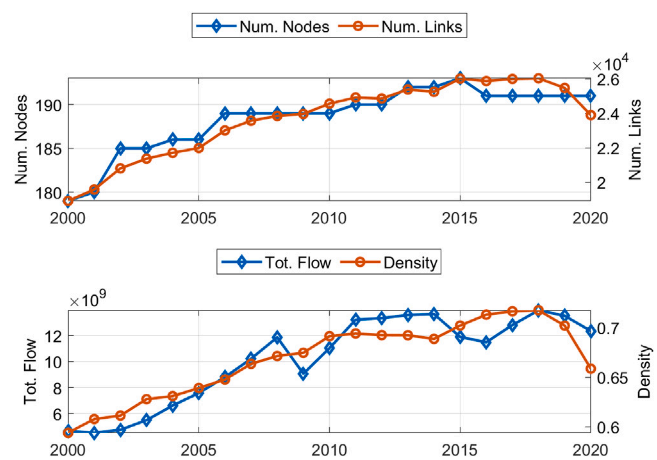

Fig. 2. Number of nodes and links together with network density and total flow. The top panel reports, in blue, the dynamics of the number of nodes involved in trade relationships (left y-axis) and the number of links in red (right y-axis). Similarly, the bottom panel shows, in blue, the total flow, i.e. the sum of network weights in US dollars (left y-axis) and the network density in red (right y-axis), i.e. the number of connections over the number of possible connections. (For interpretation of the references to color in this figure legend, the reader is referred to the web version of this article.)

4. Results

4.1. Estimation results

In this subsection we present the estimation results of the proposed gravity model, starting with yearly estimates of ZIP regression models provided in Eq. (5). To show the overall magnitude of the coefficients, we firstly provide a graphical representation of the corresponding average regression coefficients reported in the left panel of Fig. 4. The estimates highlight that, on average, Gross Domestic Product (GDP) is the variable exerting the highest (positive) impact on the dependent variable, with the GDP of the destination country (GDP Dest.) being the most impactful regressor, immediately followed by the one of the source country (GDP Source). Further, we find that contiguity (CTG), common language (COML) and trade agreements (TA) also exhibit positive regression coefficients, though their impact is relatively modest. Other variables, such as population (POP) and area (AREA), have rather negligible impact, whereas few other covariates exert, on average, negative impacts on total bilateral trade, among which, the colonial relationship (COL), common currency (COMC), landlockness (LL) and, mostly, the distance between countries (DIST). Indeed, the landlockness of a country and the fact that the country itself has previously been a colony, exert a certain negative impact on the total trade of a country pair, though, as expected, the distance between countries is the most impactful factor. Despite the different data-source of international trade flow and slight variation in the estimation procedure, our results are in line with the findings of Fagiolo (2010) and Duenas and Fagiolo (2013). The right panels provide additional insights into the role of fixed effects and network structures in shaping trade relationships. The top-right panel reports the average estimated coefficients for the fixed effects model, capturing country-specific unobserved heterogeneity. The results closely mirror those of the non-structural gravity model,

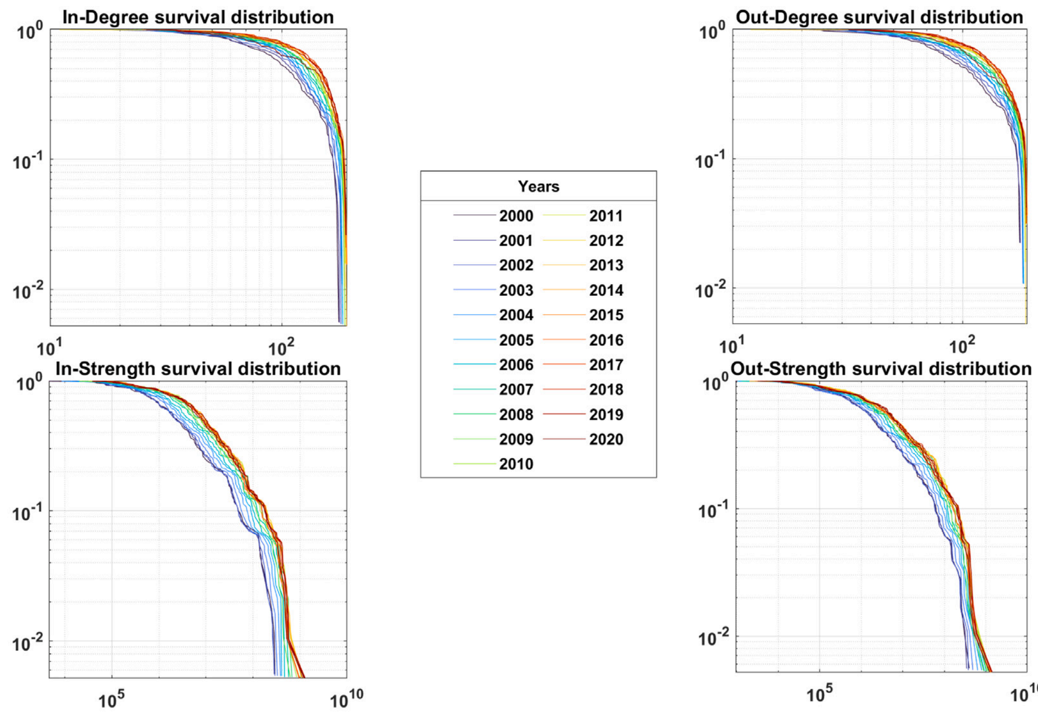

Fig. 3. Survival distributions of in- and out- degree and strength. The figure reports the yearly log–log survival functions associated with the ITN in- and out- degree (top panels) and strength (bottom panels).

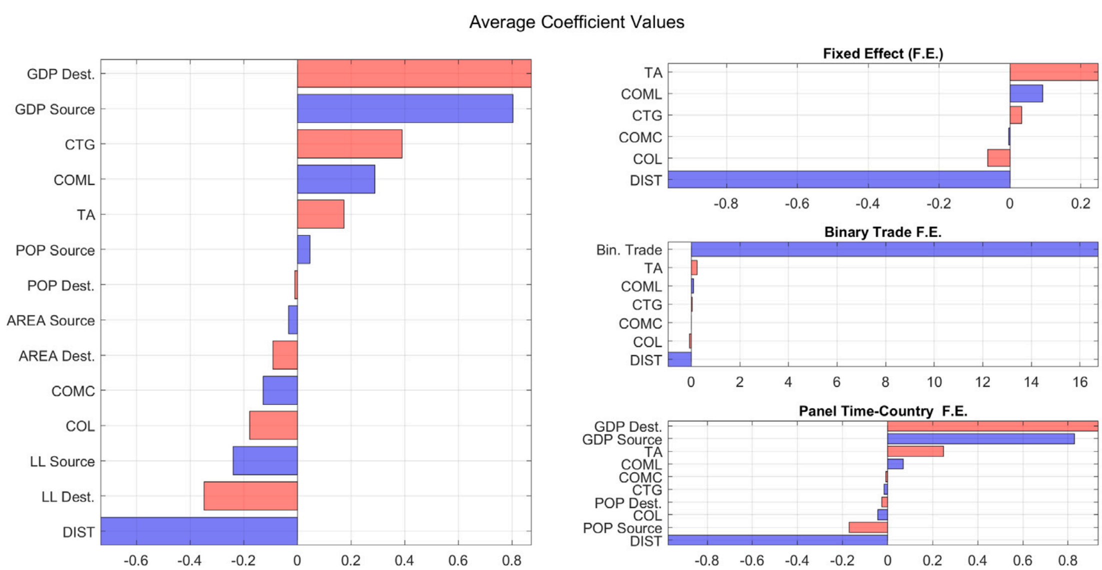

Fig. 4. Average regression coefficients related to the estimation of the models. The left panel of the figure shows the average values of regression coefficients obtained with the PPML estimation method. The length of the each bar is proportional to the value of the related coefficient reported on the *x*-axis. The variable names are reported on the *y*-axis. The top-right panel shows the average estimated values of the fixed effect model coefficients, while the central-right panel highlights the estimation outcomes for the fixed effect gravity model accounting also for the binary trade network structure. Finally, the bottom-right panel reports the estimated coefficients for the panel regression with country and time fixed effects.

with trade agreements (TA) and common language (COML) exhibiting positive effects, while distance (DIST) remains the most significant negative determinant. The central-right panel extends the analysis by incorporating a binary trade network structure into the fixed effects gravity model. The estimation highlights the importance of the extensive margin of trade, as reflected by the large coefficient on the binary trade variable, while the relative influence of other determinants remains consistent with the previous specifications. Furthermore, the comparison between the average coefficients obtained from the cross-sectional gravity estimation, shown in the left panel of the figure, and those derived from the panel specification with country and time fixed effects, reported in the bottom-right panel, reveals a strong degree of consistency. The two approaches yield remarkably similar results in terms of both the sign and the relative magnitude of the key explanatory variables. In particular, the main economic determinants of trade flows, such as the economic size of the trading partners, are confirmed to play a central role in both specifications. The positive impact of GDP variables remains robust when moving from a cross-sectional framework to a panel setting that controls for unobserved heterogeneity at the country and time level. Similarly, the well-established negative effect of geographical distance on trade volumes remains clearly identifiable and comparable across both approaches, reaffirming its fundamental importance as a trade barrier. While the cross-sectional estimates capture average relationships across all observations, the panel estimation allows for controlling unobserved, time-invariant country characteristics and common shocks. Despite these additional controls, the main coefficients remain stable, underscoring the robustness of the underlying relationships. Some differences naturally emerge in variables that may be partially absorbed by fixed effects, as expected in a panel framework. Nevertheless, the persistence of key patterns across both estimation strategies strengthens the confidence in the validity of the gravity model results and confirms the economic interpretation derived from the cross-sectional analysis.

Finally, to validate our findings, we also perform alternative estimations of Eq. (5) using other relevant econometric approaches discussed in the literature (see e.g. Linders and De Groot, 2006). These approaches include standard ordinary least squares (OLS) applied to the log-linearized form, replacing zeros with a small constant, and the Poisson model, as it ensures that the network total weight is maintained. We report in Appendix results showing the average values of the estimated coefficients obtained by employing standard OLS and Poisson models.

In Fig. 5, we report the evolution of the regression coefficients over time, together with their standard errors. Overall, the outcome observed for the average coefficients is confirmed for the variables exerting relatively high impacts on bilateral trade flows: the positive relation with the GDP of the destination and the origin countries and the negative one with the geographical distance. Moving to trends, we observe the coefficients associated to GDPs decreasing until 2010, followed by a small rise and a relative stability around values slightly lower than the starting ones. The values of the coefficient related to the distance, instead, keeps decreasing over time. In the same figure, on the top right panel, we report the coefficients related to the contiguity dummy (CTG), which show a clear decreasing trend, and the behavior of the dummy variable associated to common language between countries (COML), also decreasing over time. The coefficients associated to the variables common currency (COMC) and colony (COL) are relatively low and stable over time. Dummies indicating landlocked origin (LL Source) and destination countries (LL Dest.), having a negative effect on trade bilateral flows, exhibit a diminishing impact over time. Similarly, the estimated parameters associated to the area of the destination country (AREA Dest.) are negative and slightly decreasing in absolute value over time. Most of the remaining coefficients fluctuate around zero, becoming statistically significant only during specific years, suggesting a very mild impact of these variables on the total trade flows between country pairs.

In the context of estimating a gravity model using PPML, the computation of standard errors is crucial, particularly due to the presence of cross-sectional dependence in trade data (see Conley et al., 2023). To account for cross-sectional dependence, we compute standard errors correcting for spatial correlation by weighting residual interactions based on bilateral distances. This ensures that geographically proximate trade relationships are properly captured. Standard errors confirm the statistical significance of the regression coefficients for the whole period.

For the subsequent analysis, our primary focus will be on the fitted values of trade flows derived from gravity models. These fitted values serve as a key component for the modularity null model defined with the OT-gravity approach. Therefore, in Fig. 6, we present yearly correlation between fitted values obtained from gravity models with and without fixed effects, considering both cross sectional and panel regressions. The consistently high correlation, ranging from a peak of 0.95 in the early 2000s to a minimum of 0.895 in 2020, demonstrates a strong similarity between model specifications. This robustness in correlation suggests that the predictions of trade flows remain generally stable, irrespective of model specifications. The temporal consistency of correlations is particularly important for ensuring the validity of community detection analysis. Consequently, the high degree of similarity between the fitted values from all specifications provides a solid foundation for the modularity null model and supports the robustness of the conclusions drawn from the OT-gravity approach.

4.2. Community detection results

This subsection is devoted to the investigation of the community structure of the ITN based on the modularity function obtained with the introduction of the proposed benchmark model. In Fig. 7 we show the value of the modularity for each year of the sample and for two choices of the null model in Eq. (1): (i) the NG modularity and (ii) the OT-gravity modularity, for different values of the entropy parameter γ. At the bottom of the figure, we report the yearly difference between the two modularities for the whole period.

Results clearly show that the modularity obtained via the OT-gravity method is consistently higher than that retrieved with the standard NG model, while values associated to different γ in the OT-gravity model are close to each other. Indeed, we register an average gain in modularity of more than 10% across the observed time points when the OT-gravity model is employed against the standard modularity null model. This confirms that a null model accounting for exogenous economic factors as constraints produces a higher-quality partition of the network with respect to a model constraining for local endogenous quantities, such as the node strength.

We investigate in Fig. 8 the distribution of nodes across communities by means of violin plots, with the violin shape representing the community distributions. The figure reports four subplots, each associated with the partitions obtained from the NG null model (top panel) and the OT-gravity method for different values of the entropy parameter γ. The number of communities is represented on the y-axis while the width of the violin is proportional to the number of nodes composing each community. To provide an intuition, a very narrow and stretched violin suggests a high number of communities, each one populated by a small number of countries. On the contrary, wider and shorter violins indicate the presence of a few communities composed of a large number of nodes. A number of observations can be drawn from Fig. 8. Firstly, the NG modularity yields a higher number of communities compared to our OT-gravity method and across various alternative configurations (i.e., value of the entropy parameter γ), specifically at the beginning and at the end of the sample. This pattern is more evident when the entropy parameter is low and therefore the impact of the gravity estimate in the null model is high. Secondly, despite notable disparities between the methods, discernible patterns emerge in the number and size distribution of communities across the two alternatives. In fact, we observe a few communities counting most of the nodes, while the majority of the partitions has small size. Additionally, while the Global Financial Crisis period (2008–2009) has produced a reduction in the number of communities, the trade slow-down of 2015 has generated a more fragmented network, characterized by a higher number of communities. In summary, the observed mesoscale organizational structure of the ITN, identified through modularity maximization when the NG and the OT-gravity null models are employed, appears relatively consistent, with a slight difference in the number of communities.

In order to compare the partitions of nodes provided by the different models, we make use of measures from information theory. In particular, we consider two quantities: the normalized mutual information and the normalized variation of information (Expert et al., 2011). The former quantifies the common information between two partitions results, emphasizing their similarity. The latter measures the overall dissimilarity by considering both shared and exclusive information. In formulas, the normalized mutual information reads as:

$$NMI(\mathcal{P}_1, \mathcal{P}_2) = \frac{I(\mathcal{P}_1, \mathcal{P}_2)}{\sqrt{E(\mathcal{P}_1)E(\mathcal{P}_2)}},$$

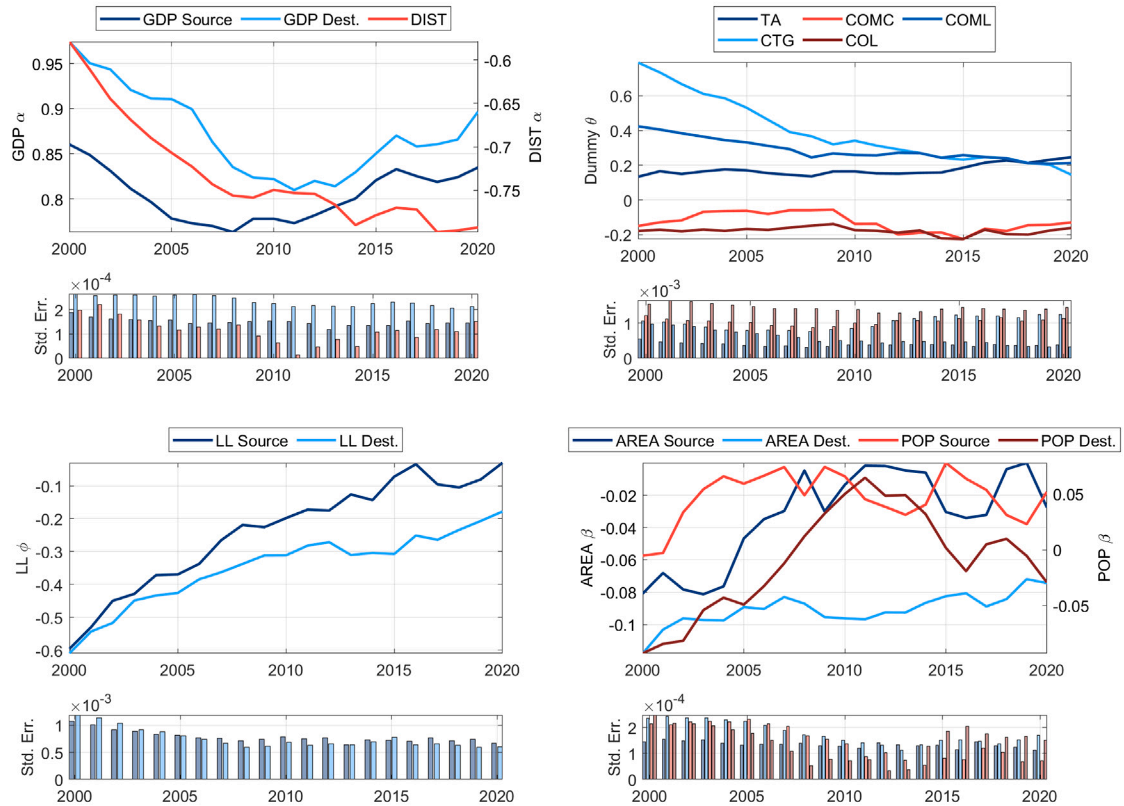

Fig. 5. Regression coefficients associated to the PPML estimation over time. The figure shows the evolution of the regression coefficients associated to each variable along with the respective standard error. Variable names are reported in the title of each subplot. The right and left y-axes report the magnitude of the coefficients.

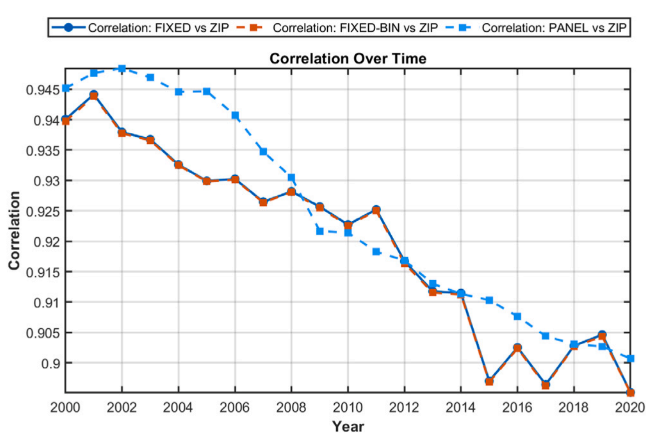

Fig. 6. Yearly correlation between fitted values from gravity models with and without fixed effects. The figure illustrates the annual correlation between fitted trade flow values derived from gravity models with and without fixed effects (also including the network binary structure) along with the panel regression with both country and time fixed effects. The correlations range from 0.95 in the early 2000s to 0.895 in 2020, and demonstrate strong similarity between the model specifications.

where $I(\mathcal{P}_1, \mathcal{P}_2)$ is the mutual information between the two partitions $\mathcal{P}_1$ and $\mathcal{P}_2$, while $E(\cdot)$ represents the entropy. The normalized variation of information instead is defined as follows:

$$VI(\mathcal{P}_1, \mathcal{P}_2) = \frac{E(\mathcal{P}_1) + E(\mathcal{P}_2) - 2I(\mathcal{P}_1, \mathcal{P}_2)}{\log(N)}.$$

We present in Fig. 9 the evolution of normalized mutual information and normalized variation of information over time. Both quantities range between 0 and 1: the higher the normalized mutual information (the lower the normalized variation of information), the higher the similarity between the two partitions. A visual inspection of Fig. 9 reveals that the normalized mutual information and the normalized variation of information are relatively similar for different values of the entropy parameter γ, with the model associated to the lowest γ being the one differing at most from the standard model (as previously observed for the community distributions). In fact, when increasing the entropy parameter, the OT-gravity based methodology tends to the NG benchmark. The normalized mutual information suggests that the shared information between the results of the NG model and OT-gravity based method is quite low when considering the beginning of the sample (accordingly, the normalized variation of information is relatively high). However, it further increases from 2002 to decline in 2015, rises again and falls down in the year 2020, in concurrence with the COVID-19 outbreak. This outcome indicates that, while the dot-com bubble of the early 2000, the trade slow-down of 2015 and the COVID-19 outbreak of 2020 have yielded a significant disparity between the emerging partitions generated by the two approaches, the Global Financial Crisis seems to have affected more weakly the community structure compared to the other events. This translates into the fact that, in the latter case, constraining for economic factors does not influence the mesoscale organization of the ITN allegedly because of other elements, such as financial aspects, which might drive the network behavior.

For sake of completeness, we present in Appendix a similar analysis, with the gravity equation being estimated with the inclusion of fixed effects, panel regression and through conventional OLS and Poisson regression models.

4.3. Community structure and financial indicators

In this subsection, we aim to investigate whether and to what extent the ITN community structure is related to some additional factors, other than those included in the OT-gravity null model of the modularity

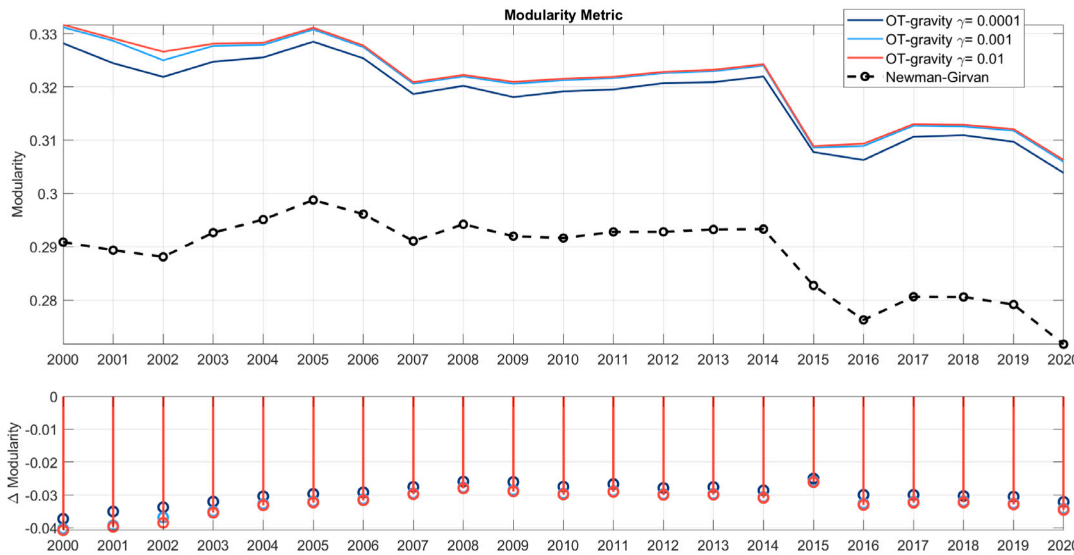

Fig. 7. Modularity dynamics for different null models. The figure reports, in the top panel, the evolution of the modularity obtained for the NG benchmark model (black) and for the OT-gravity alternatives, computed with different entropy parameter values. The bottom panel shows the difference in modularity between the two models. The legend associates colors with the respective model.

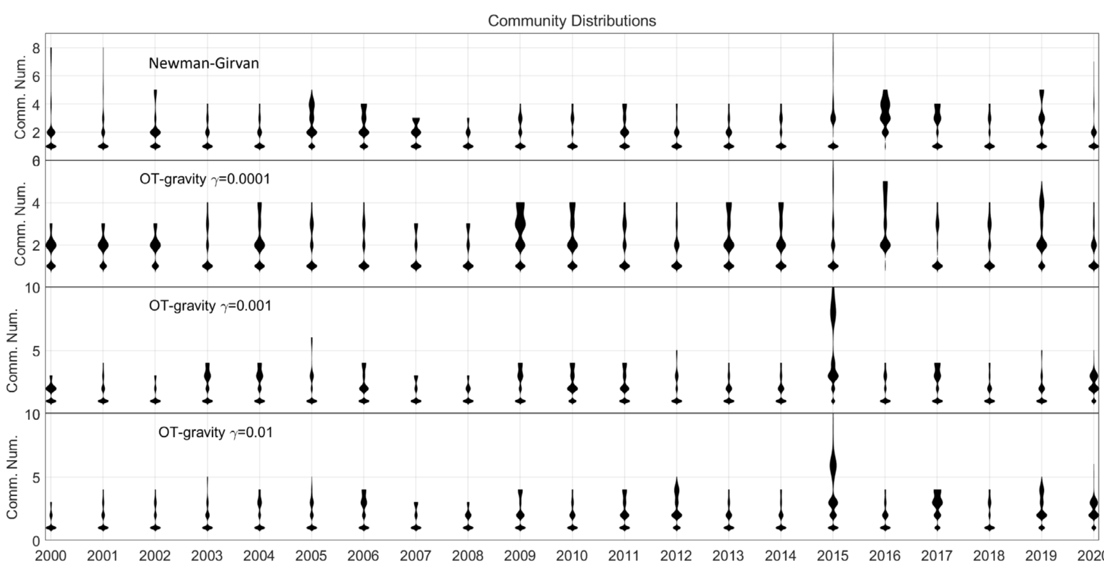

Fig. 8. Violin plot of community distribution. The figure shows the yearly community distribution through violin plots. The top row is associated with the NG model while the others represent outcomes for the OT-gravity alternatives for different values of the entropy parameter γ. The y-axis reports the number of communities for each year while the violin shape represents the community distributions.

function. Consequently, a key question revolves around the identification of *extra* drivers behind the emerging partitions. Here, we postulate the existence of a possible link between the financial development of countries and the mesoscale structure of the ITN. Indeed, some scholars have explored to what extent financial factors influence the configuration of the trade balance, emphasizing the significance of financial sector development in economic progress and bilateral trade flows (Beck, 2002; Leibovici, 2021).

In addressing the role of financial development in the community structure of the ITN, it is essential to recognize the potential for omitted-variable bias in the analysis. Omitted-variable bias arises when important factors influencing the relationship between financial development and trade flows are not included in the model, which may lead to misleading or incomplete conclusions. For instance, other unobserved factors such as political stability, geographic proximity, or cultural ties could also play a significant role in shaping trade relations and the emerging community structure. However, it is important to note that our analysis mitigates such concerns by employing a fixed effects estimation. This approach controls for unobserved heterogeneity across countries that remains constant over time, effectively accounting for time-invariant factors that could otherwise lead to omitted-variable bias. The robustness of our results to this specification further strengthens the argument that the observed relationships between financial development and the ITN community structure are not spurious due to omitted variables.

We leverage data from the Financial Development Index database compiled by the International Monetary Fund, which contains a set of indices characterizing the degree of development of financial institutions and financial markets in terms of their depth, access, and efficiency.[9] In particular, we consider nine indicators at different level

[9] https://data.imf.org/?sk=f8032e80-b36c-43b1-ac26-493c5b1cd33b&sid=1480712464593

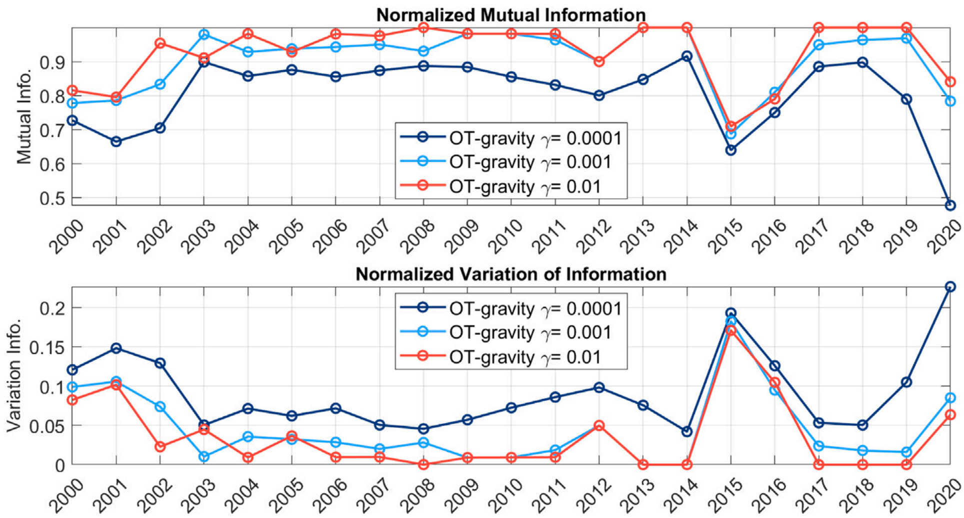

Fig. 9. Normalized mutual and variation of information. The figure reports the evolution of normalized mutual information (top) and normalized variation of information (bottom) to assess the distance between partitions provided by modularity maximization obtained with the standard NG model and that of the OT-gravity null model. The legend associates colors with the respective model.

of aggregation. The *Financial Development* index (FD) is an aggregate of two sub-indices, namely the *Financial Institutions* index (FI) and the *Financial Markets* index (FM), that are, in turn, aggregation of other sub-indices according to the following list. The FD includes:

- The *Financial Institutions* index (FI), composed by:
  - The *Financial Institutions Depth* index (FID), which includes metrics such as bank credit to private sector as a percentage of GDP, pension fund and mutual fund assets to GDP, and insurance premiums (life and non-life) to GDP;
  - The *Financial Institutions Access* index (FIA,) which measures bank branches and ATMs per 100,000 adults;
  - The *Financial Institutions Efficiency* index (FIE), which considers banking sector metrics, including net interest margin, lending-deposits spread, non-interest income to total income, overhead costs to total assets, return on assets, and return on equity.
- The *Financial Markets* index (FM), which comprises:
  - The *Financial Markets Depth* index (FMD), which includes metrics such as stock market capitalization to GDP, stocks traded to GDP, international government debt securities to GDP, and total debt securities of financial and non-financial corporations to GDP;
  - The *Financial Market Access* index (FMA), which measures the percentage of market capitalization outside the top 10 largest companies and the total number of debt issuers (domestic and external, non-financial and financial corporations) per 100,000 adults;
  - The *Financial Markets Efficiency* index (FME), which focuses on the stock market turnover ratio (stocks traded to capitalization).

To provide a preliminary inspection on how financial indices are related to communities, we report in Fig. 10 three box-plots that highlight how financial variables are distributed across partitions in different years, namely in 2000, 2010 and 2016. We observe that, for some variables, box-plots are mostly overlapped, whereas for others there is a minimal overlap, suggesting covariates play a role in explaining community partitions. This behavior is more evident for the FDI, the FIA and the FI indices.

To quantify the relationship between financial factors and the community structure, we first compute pairwise financial distances between countries i and j using multiple distance metrics. Given the $N \times M$ matrix $\mathcal{Z}$, where each row corresponds to the $1 \times M$ vector of financial features for a country, we compute distances between vectors z_i and z_j using the following measures. The Euclidean distance is given by:

$$d_{i,j} = (z_i - z_j)(z_i - z_j)'. \tag{19}$$

The cosine distance is defined as:

$$d_{i,j} = 1 - \frac{z_i z_j'}{\sqrt{(z_i z_j')(z_i z_j')}}. \tag{20}$$

The correlation-based distance is given by:

$$d_{i,j} = 1 - \frac{(z_i - \bar{z}_i)(z_j - \bar{z}_j)'}{\sqrt{(z_i - \bar{z}_i)(z_i - \bar{z}_i)'}\sqrt{(z_j - \bar{z}_j)(z_j - \bar{z}_j)'}}, \tag{21}$$

where $\bar{z}_i$ and $\bar{z}_j$ denote the mean financial feature values of countries i and j, respectively. Next, we aggregate these pairwise financial distances at the community level, as derived from the OT-gravity approach. This aggregation enables a comparative analysis of both within-community and between-community financial distances. Fig. 11 presents a detailed visualization of these financial distances in the ITN, with each subplot corresponding to a different distance metric. Across all distance metrics, a consistent pattern emerges: within-community financial distances (blue bars) tend to be lower than between-community distances (orange bars), especially after 2003. This observation supports the hypothesis that financial factors influence the mesoscale structure of the ITN, as countries within the same community exhibit greater financial similarity.

To assess whether the differences between within-community and between-community financial distances are statistically significant, we perform three different tests, i.e. the Kolmogorov–Smirnov (KS) test, the standard t-test, and the Mann–Whitney U test. The KS test evaluates whether the distributions of the two groups differ significantly. The t-test assesses differences in means under the assumption of normality, while the Mann–Whitney U test provides a non-parametric alternative for comparing distributions. Table 2 reports the results. Across all distance metrics, the KS test statistics are relatively high, with p-values below 0.05, indicating significant distributional differences. The t-tests yield negative test statistics, confirming that within-community distances are significantly lower than between-community distances, with p-values below 0.001. The Mann–Whitney U test further corroborates these findings, supporting the hypothesis that financial similarity plays a role in shaping community structure of the ITN network.

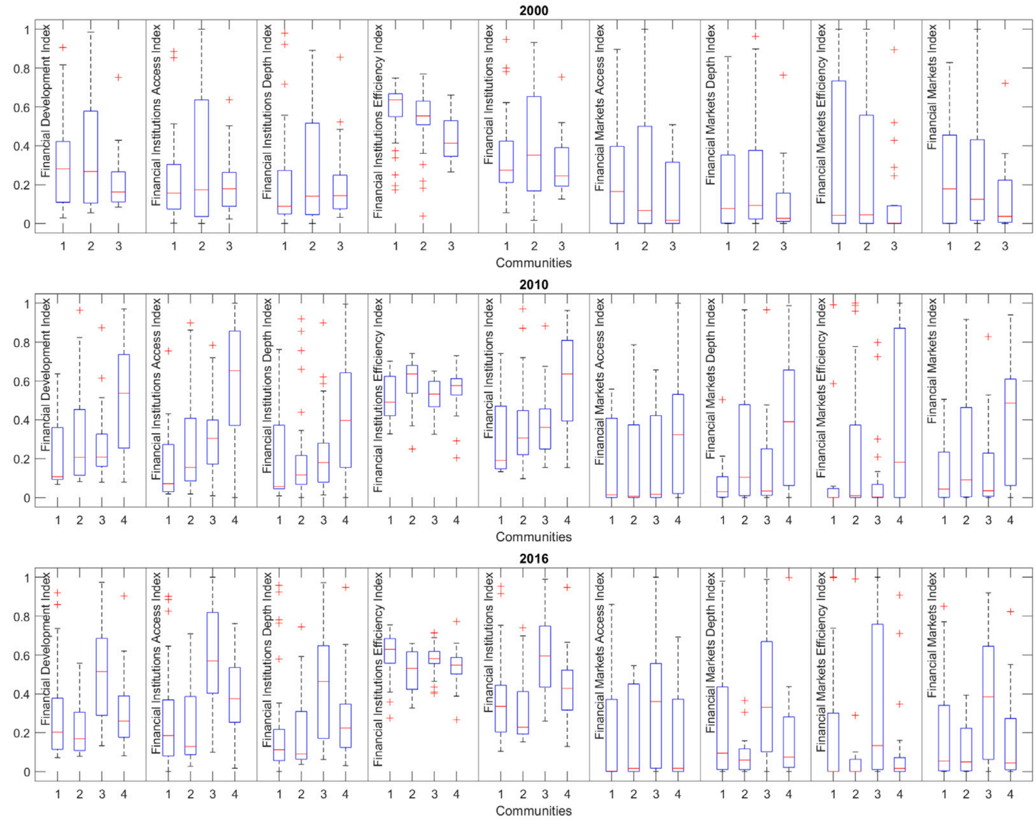

Fig. 10. Box-plot of financial indices across communities. The figure shows three box-plots which describe how financial variables are associated with different communities in 2000, 2010 and 2016. The partitions are computed with the OT-gravity modularity for $\gamma = 0.001$.

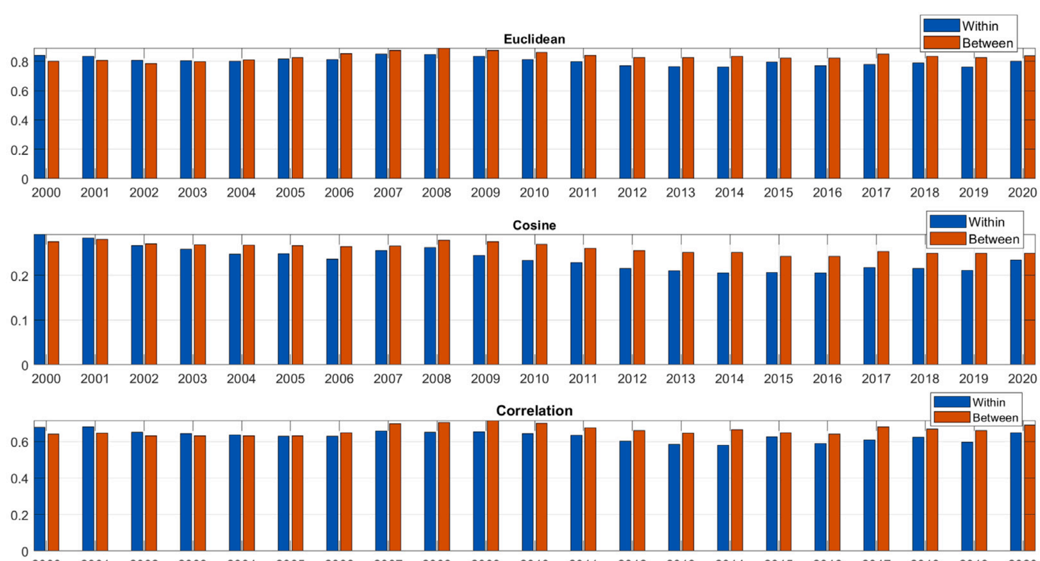

Fig. 11. Average financial distances within and between communities in the ITN. Blue bars indicate within-community distances, while orange bars represent between-community distances. The lower within-community distances across all dimensions suggest that financial similarities contribute to the formation of network communities. (For interpretation of the references to color in this figure legend, the reader is referred to the web version of this article.)

To reinforce the findings from previous analysis, we conduct a multiclass classification task using machine learning models. Our objective is to evaluate the models' capability to forecast class labels derived from the community partitions, based on feature vectors represented by financial development indices. Given our interest in elucidating a potential rationale behind the emerging mesoscale structure of the ITN under economic constraints, we perform in-sample classifications. This entails training the models and subsequently assessing their performance on the same dataset. We utilize three distinct machine learning models, namely, discriminant analysis, support vector machine, and classification trees (Klecka, 1980; Cristianini and Shawe-Taylor, 2000; Breiman, 2017). For each model, we conduct two separate experiments. Employing the same set of covariates, i.e., the financial development indices, we initially designate the partitions obtained through the

Table 2
Statistical tests comparing within-community and between-community financial distances. The table shows the test statistics and p-values of the Kolmogorov–Smirnov (KS) test, the standard t-test, and the Mann–Whitney U test to compare the financial distances obtained through the Euclidean, cosine and correlation-based distance metrics.

	Euclidean	Cosine	Correlation
KS Statistic	0.52381	0.61905	0.47619
KS p-value	3.59×10^{-3}	2.92×10^{-4}	1.08×10^{-2}
t-test Statistic	−3.6291	−3.8681	−3.7016
t-test p-value	7.98×10^{-4}	3.95×10^{-4}	6.45×10^{-4}
Mann–Whitney U Statistic	330	320	331
Mann–Whitney U p-value	2.34×10^{-3}	9.83×10^{-4}	2.54×10^{-3}

standard NG modularity as the target variable. Subsequently, we use the communities derived from the OT-gravity method as the target variable. Our hypothesis posits that the covariates exhibit enhanced discriminative power when considering the outcomes of the OT-gravity method. In essence, these covariates should exhibit higher variations across partitions obtained through the OT-gravity method, compared to standard modularity, thereby yielding more precise predictions. As a metric for evaluating the performance of the classification models, we compute the F1-score, which combines precision and recall into a single value. We rely on the F1-score since it accounts for class imbalances and it considers both false positives and false negatives, thus providing a more comprehensive evaluation of the model's ability to correctly classify instances from different classes. Fig. 12 reports the percentage difference in the F1-score metric as in Eq. (22), which reflects the explanatory capacity of financial development indices in classifying the partitions generated by the OT-gravity method versus those derived from the standard NG modularity:

$$\Delta F1_{\gamma} = \frac{F1^{OT}_{\gamma} - F1^{NG}}{F1^{NG}} * 100. \tag{22}$$

Each panel represents the outcome of a specific machine learning model, as indicated in the respective title. Overall, the three models yield results which are consistent, showing a higher F1-score difference during crisis phases. In fact in these periods the OT-gravity partitions largely differ from the communities arising from the standard modularity approach. In particular, in accordance with the results on theoretical information (see Fig. 9), the F1-score difference is relatively high during the dot-com bubble of the early 2000s, the trade slowdown of 2015, and the COVID-19 outbreak of 2020, whereas the Global Financial Crisis of 2008–2009 appears to have had no discernible impact on the model performance. This behavior is more evident for the OT-gravity model when the entropy parameter is set to $\gamma = 0.0001$. On the other hand, during business as usual times, financial development covariates do not exhibit high discriminatory power when comparing partitions.

4.4. Scenario analysis

In this subsection we conduct a policy experiment to assess if and how shocks involving key economic variables of selected sets of countries affect the community structure of the ITN. Policy and scenario analysis allow decision-makers to explore potential outcomes, assess risks, and develop informed strategies against uncertainties around the global structure of trade.

The standard NG modularity function, which consists of a benchmark model based on purely endogenous local network constraints (such as the degree or strength), allows to make considerations only in terms of the interaction structures, and not in terms of associations with exogenous economic factors. Specifically, it is possible to analyze variations in the community structure determined by modifications of the network structure itself, but not to provide the functional relationships describing such variables interactions. Using estimates derived from the gravity equations within the null model of the modularity function can significantly enhance our ability to simulate various scenarios and analyze potential policy impacts (Bollen et al., 2020).

In particular, since the trade data we consider only covers bilateral flows until 2020, we decide to conduct a scenario analysis on the impact of a large, exogenous shock to the economy such as the COVID-19 outbreak. In particular, we produce two scenarios related to the COVID-19 pandemic. In the first scenario we simulate a recovery from the negative economic impact of the pandemic by keeping fixed the regression coefficients of the year 2020 and by considering covariates for the year 2021, thus estimating import–export relationships for such year and the corresponding emerging community structure. In the second scenario, we hypothesize that a group of countries does not recover from the shock. We simulate such scenario with a 10% GDP reduction for two set of countries (separately): G7 economies (United States, Canada, United Kingdom, Germany, Italy, Japan and France) and the BRICS countries (Brazil, Russia, India, China and South Africa).[10]

In Fig. 13 we present metrics related to the emerging partitions of the ITN in the scenario analysis. In particular, we show the modularity values, the number of communities and two information theory criteria to compare network partitions. We employ the recovering scenario as benchmark (No Shock) and we report the outcome of the GDP reduction for G7 countries in the upper panel of Fig. 13, while in the bottom panel we show the results for the BRICS countries. We observe, besides a slight decrease in the modularity values, an increase in the number of communities. In both cases, theoretical information measures confirm the dissimilarity of the resulting partitions.

Fig. 14 shows the ITN community structure of the recovery scenario for 2021 (No Shock) and those emerging when simulating the occurrence of negative GDP shocks. In the absence of the GDP shock (Fig. 14, top panel), three communities arise: (i) the North and Central American countries; (ii) the South America, Central Africa, Australia, Middle-East, South and East Asia countries; (iii) European countries, Russia, North and South Africa. When shocks are introduced, we observe an increase in the number of communities with countries forming new geographically-oriented clusters. In particular, for the G7 shock (Fig. 14, bottom left panel), the Central and South African countries merge in a new community, and the same occurs for Central American countries. Instead when shock affects the BRICS economies (Fig. 14, bottom right panel) the European community emerges.

5. Concluding remarks

In this paper, we have proposed a novel approach to model the community structure of the ITN. By introducing estimates derived from the gravity equations in the benchmark model of the modularity function, we have uncovered the emerging mesoscale structure of the worldwide import–export trade network while accounting for major economic factors. Optimal Transport theory serves as a methodology for constructing the benchmark null model, incorporating trade flow estimations while preserving the same constraints of the standard modularity framework.

We have firstly estimated the gravity equations using zero-inflated Poisson pseudo-maximum likelihood to have yearly estimates of trade flow relationships as a function of socio-economic factors. The signs and magnitudes of the coefficients align consistently with those reported in the related literature. Trade flows exhibit positive associations with factors such as country GDP, the presence of trade agreements, shared borders and common language. Conversely, a negative impact on trade flows is observed for distance, area, and the likelihood of being landlocked. We have also estimated a gravity model with fixed effects,

[10] We are aware that the GDP variable also includes net exports but, in this exercise, we assume the shock is only driven by the internal demand component.

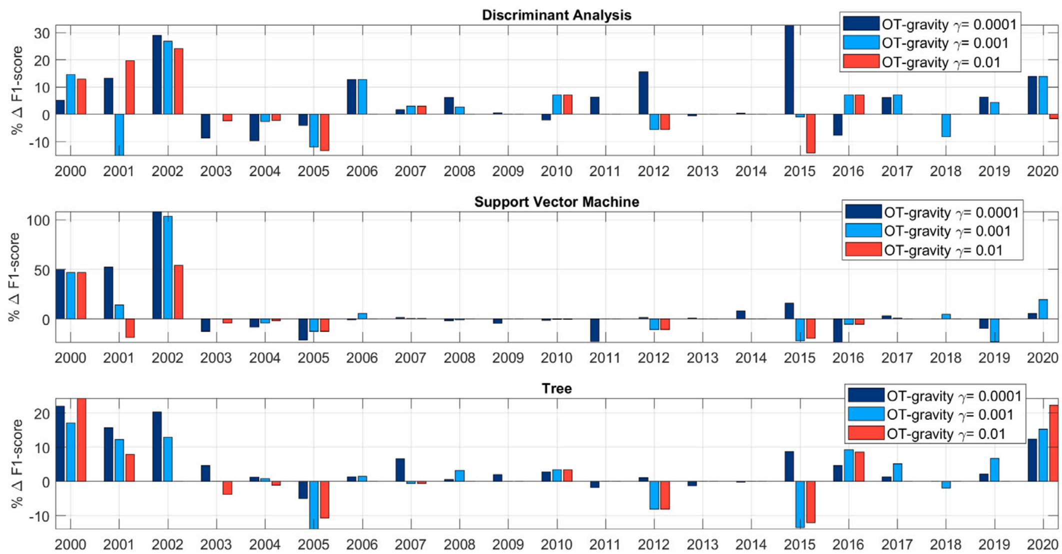

Fig. 12. F1-score percentage difference. The figure shows the percentage difference of the F1-score metric obtained when considering the explanatory power of financial development indices in classifying the OT-gravity partitions and the community structure derived from the NG modularity approach. Each panel refers to the outcome of a particular machine learning model as reported in the corresponding title.

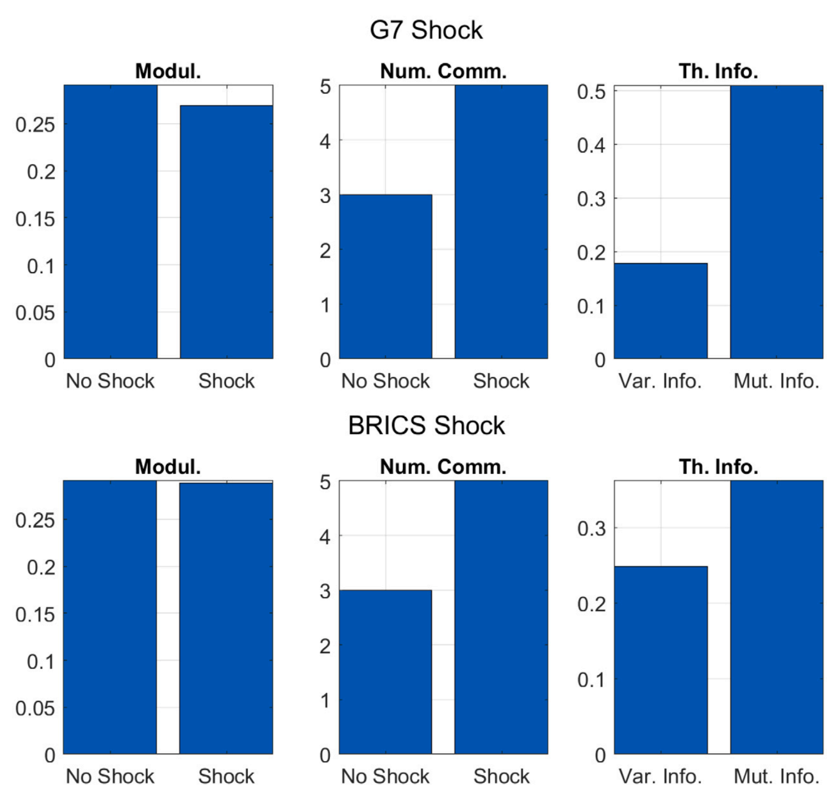

Fig. 13. Community metrics for scenario analysis. The figure reports, for the two scenario analysis, the modularity values (Modul.) along with the number of communities (Num. Comm.) and theoretical information metrics (Th. Info.), namely the normalized variation of information (Var. Info.) and the mutual information (Mut. Info.). The upper panels refer to the GDP shock to the G7 economies while lower panels show results for the BRICS shock. All the outcomes are compared against the 2021 recovery scenario (No Shock).

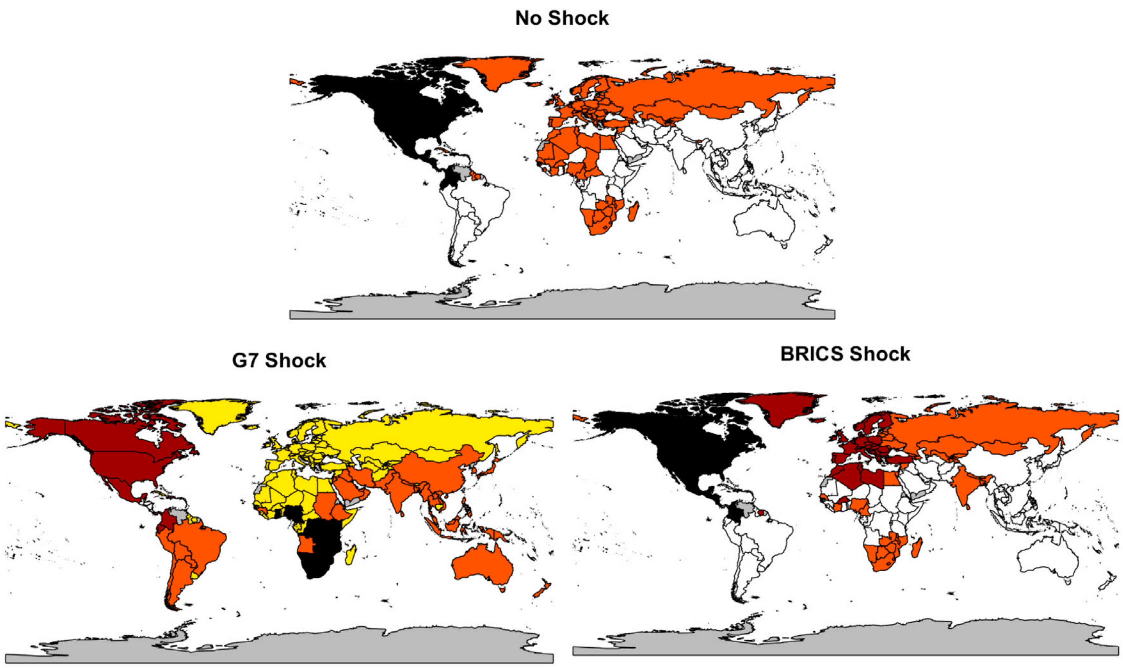

Fig. 14. Countries partitions arising from scenario analysis. The figure compares countries partitions derived from the 2021 recovery scenario (No Shock) against the shock scenario for the G7 and the BRICS economies. Black, orange, red, white and yellow colors identify the different communities while gray applies to countries with no data. (For interpretation of the references to color in this figure legend, the reader is referred to the web version of this article.)

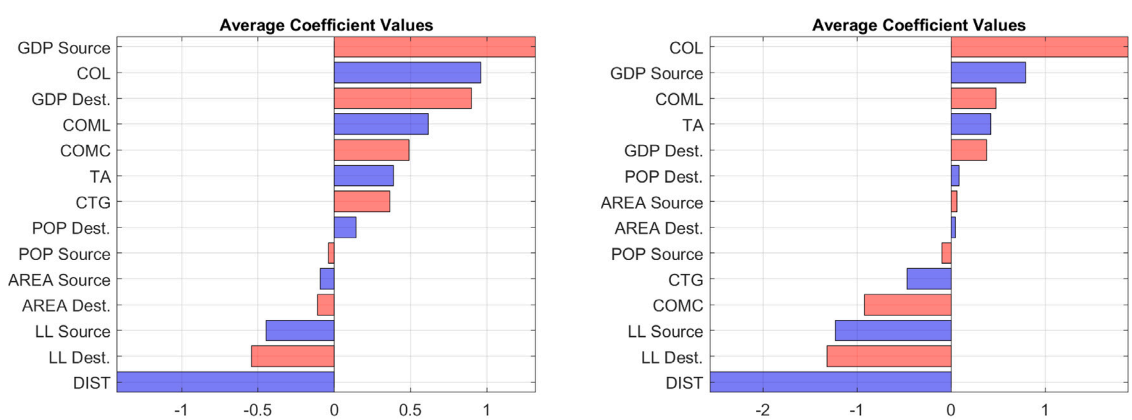

Fig. A.1. Average regression coefficient values for OLS and Poisson estimations. The figure shows the average values of regression coefficients obtained with the OLS estimation method (left panel) and with the Poisson regression (right panel). The length of the each bar is proportional to the value of the related coefficient reported on the *x*-axis. The variable names are reported on the *y*-axis.

incorporating also an additional control to account for the binary network structure. The results closely align with those of the non-structural gravity model, confirming that trade agreements and common language positively influence trade flows, while geographical distance remains the most significant negative determinant. A correlation analysis of the fitted values indicates that trade flow predictions remain stable regardless of the inclusion of fixed effects in the model specification. This stability reinforces the validity of the modularity null model and supports the robustness of the conclusions drawn from the OT-gravity approach. The inclusion of economic factors in the null model of the modularity function has been shown to provide a higher modularity metric, suggesting a better-quality partition of the network and well-defined clusters. Moreover, we have observed that a small number of communities gather the majority of nodes, while the majority of clusters are made up of only a few countries. However the standard NG model consistently yields a higher number of communities compared to the OT-gravity method across various alternative configurations.

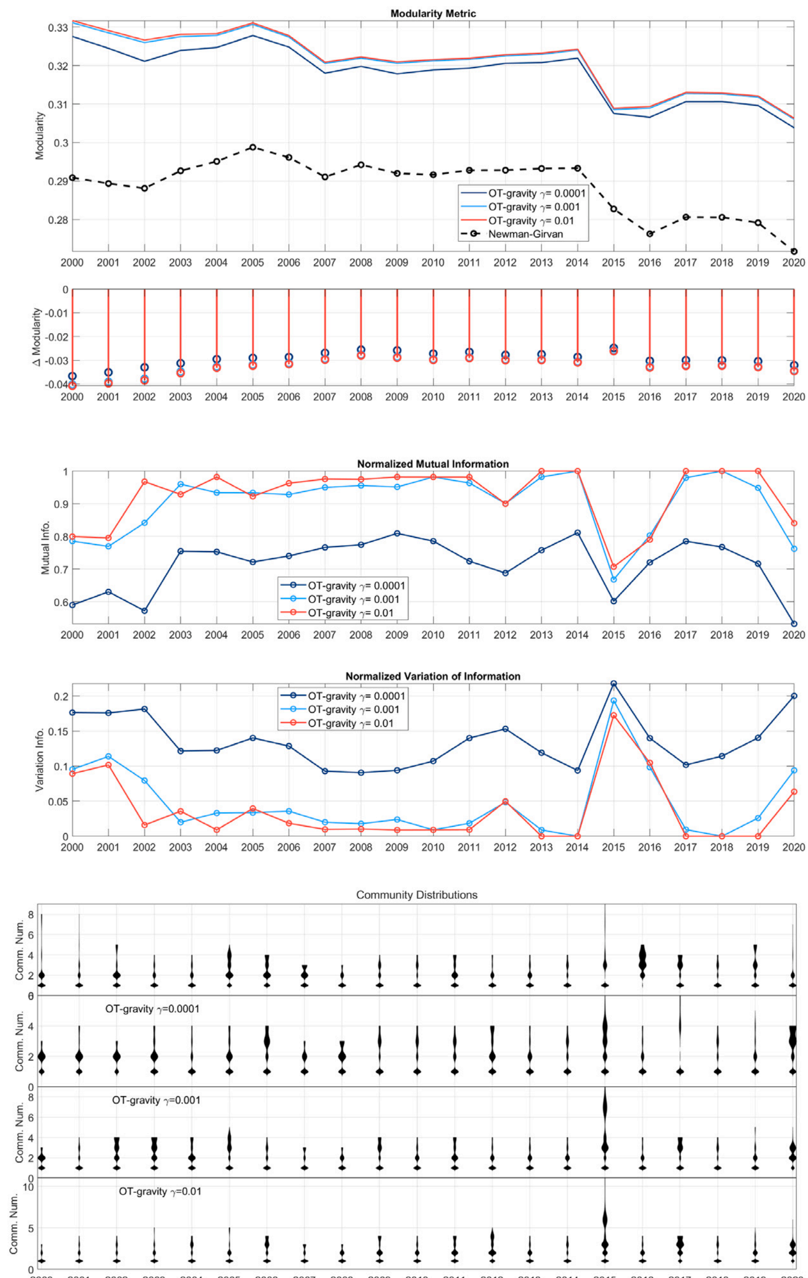

Fig. A.2. Community evaluation metrics for the gravity model estimation with fixed effects. The figure reports the evolution of some community metrics obtained with the fixed effect gravity model. In particular, the first two panels show the modularity and the change in the modularity values for the different models. Central panels show the normalized mutual and variation of information while lower panels summarize the change in the community distributions over time.

Our results have also shown that the community structure obtained by the proposed OT-gravity method can be explained by "external" financial drivers, beyond what is accounted for when deriving the emerging partitions. We find that the partitions of the ITN can be explained by the degree of financial development and, in particular, by the development of financial institutions of countries themselves. This relationship is generally stronger for what concerns extreme events such as the dot-com bubble, the 2015 trade slow-down and the COVID-19 pandemic.

Our proposal, by providing the functional relationships describing variables interactions, has allowed us to conduct scenario analysis in order to assess changes in the community structure of the ITN following global shocks in the economy. In particular, we have simulated two scenarios related to the COVID-19 pandemic, namely a recovery and a prolonged crisis due to a negative GDP shock for the G7 and BRICS economies (separately). We have observed, for the shock scenarios, an increase in the number of communities with countries forming new geographically-oriented clusters.

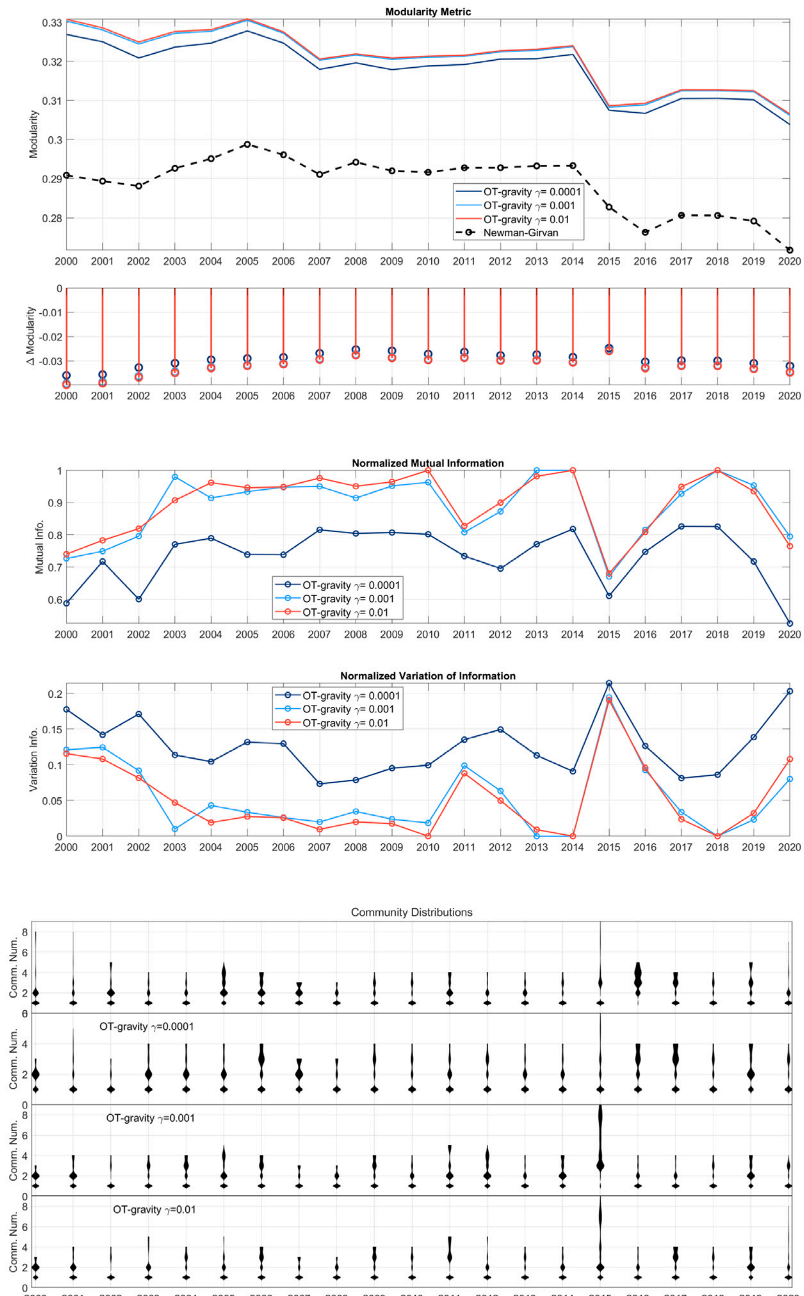

Fig. A.3. Community evaluation metrics for fixed effect estimation including the binary network structure. The figure reports the evolution of some community metrics obtained with the fixed effect gravity model which includes the binary network trade relationships. In particular, the first two panels show the modularity and the change in the modularity values for the different models. Central panels show the normalized mutual and variation of information while lower panels summarize the change in the community distributions over time.

While our approach offers valuable insights by integrating key economic factors into community detection within the ITN, several limitations warrant further discussion. First, modularity maximization for community detection comes with some notable challenge: (i) the resolution limit can strongly affect the proper identification of groups in presence of an heterogeneous distribution of cluster sizes; (ii) the lack of a clear global maximum leads to instability, as different algorithm iterations may produce different partitions; (iii) the high computational cost of finding the optimal partition requires heuristic approaches that do not always guarantee the best solution (Fortunato and Barthelemy, 2007; Good et al., 2010; Lancichinetti and Fortunato, 2011). To mitigate these issues, one can adopt multi-resolution techniques, explore alternative models like stochastic block models, consider algorithms that allow communities to overlap (see, e.g., Pecora et al. (2016), and, most importantly, interpret results with caution, as a high modularity score does not always reflect the most meaningful community structure.

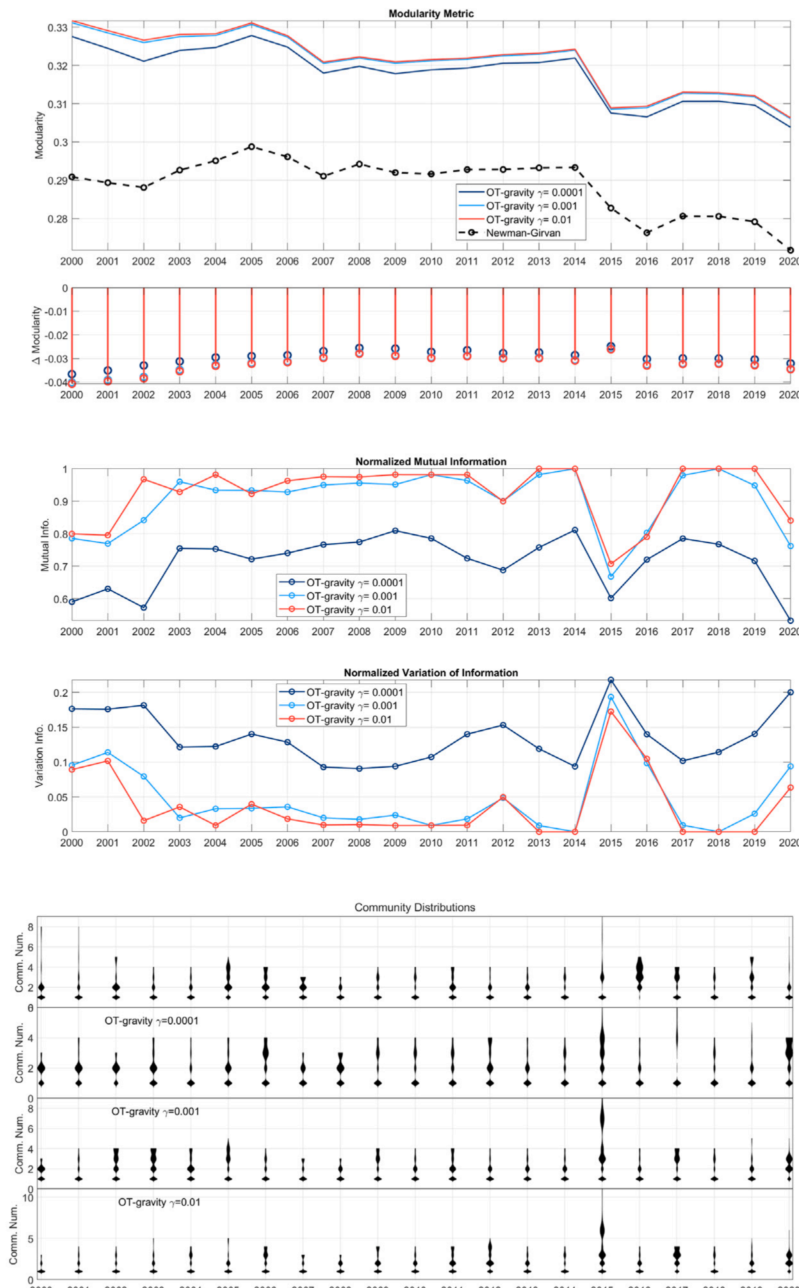

Fig. A.4. Community evaluation metrics for the gravity model estimation with panel regression. The figure reports the evolution of some community metrics obtained with the panel regression including time and countries fixed effects. In particular, the first two panels show the modularity and the change in the modularity values for the different models. Central panels show the normalized mutual and variation of information while lower panels summarize the change in the community distributions over time.

Second, although the gravity model employed accounts for standard determinants such as GDP, distance, and trade agreements, it omits potentially influential variables, including political risk, technological readiness, supply chain integration, and non-tariff barriers (Brun et al., 2005; Chaney, 2008; Luckstead et al., 2024). Incorporating firm-level data or sector-specific gravity models could also enhance the granularity of the analysis and reveal industry-specific clustering patterns. Third, the optimal transport framework used for constructing the null model introduces an entropy regularization parameter whose calibration remains non-trivial; exploring adaptive or data-driven methods for selecting this parameter could improve robustness. Finally, the estimation of trade flows through parametric models may introduce specification errors. The adoption of machine learning-based predictive models (e.g., deep neural networks or ensemble methods trained on a

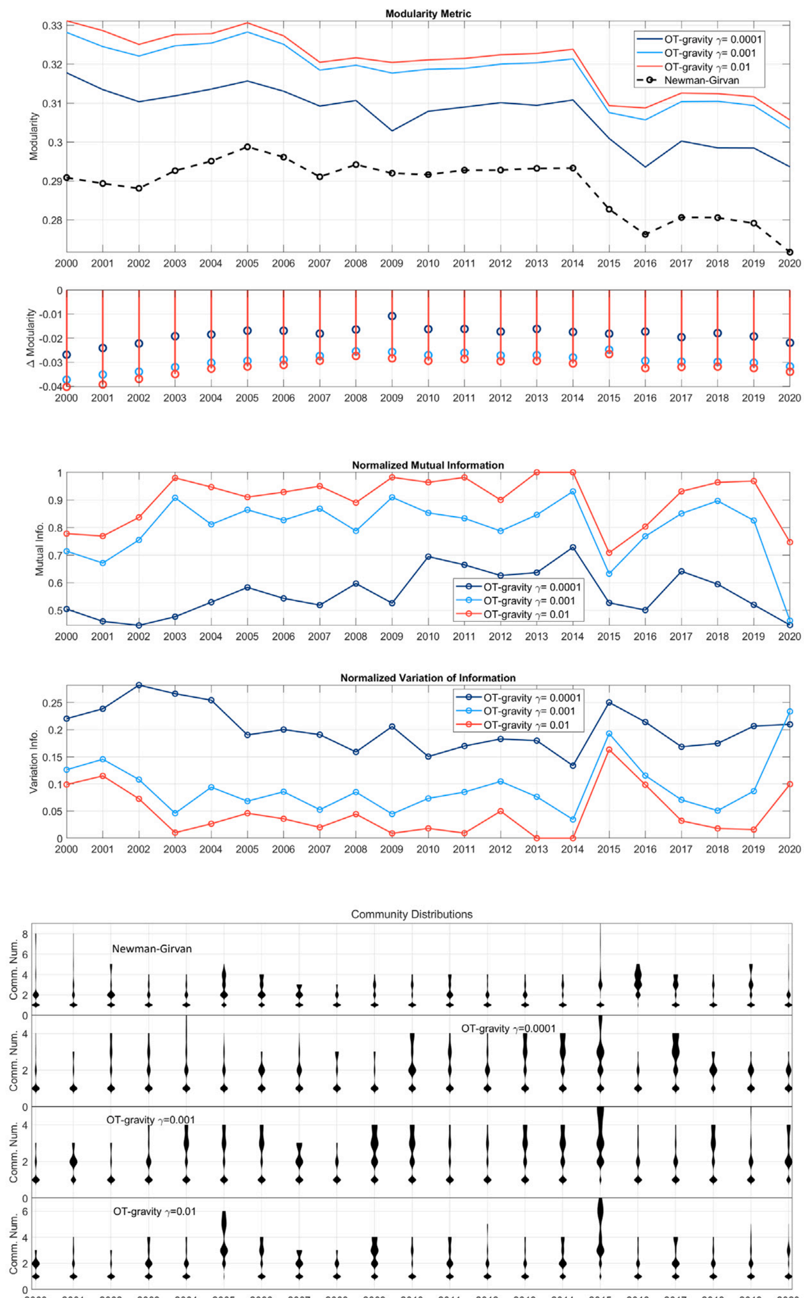

Fig. A.5. Community evaluation metrics for OLS estimation. The figure reports the evolution of some community metrics obtained with the OLS regression. In particular, the first two panels show the modularity and the change in the modularity values for the different models. Central panels show the normalized mutual and variation of information while lower panels summarize the change in the community distributions over time.

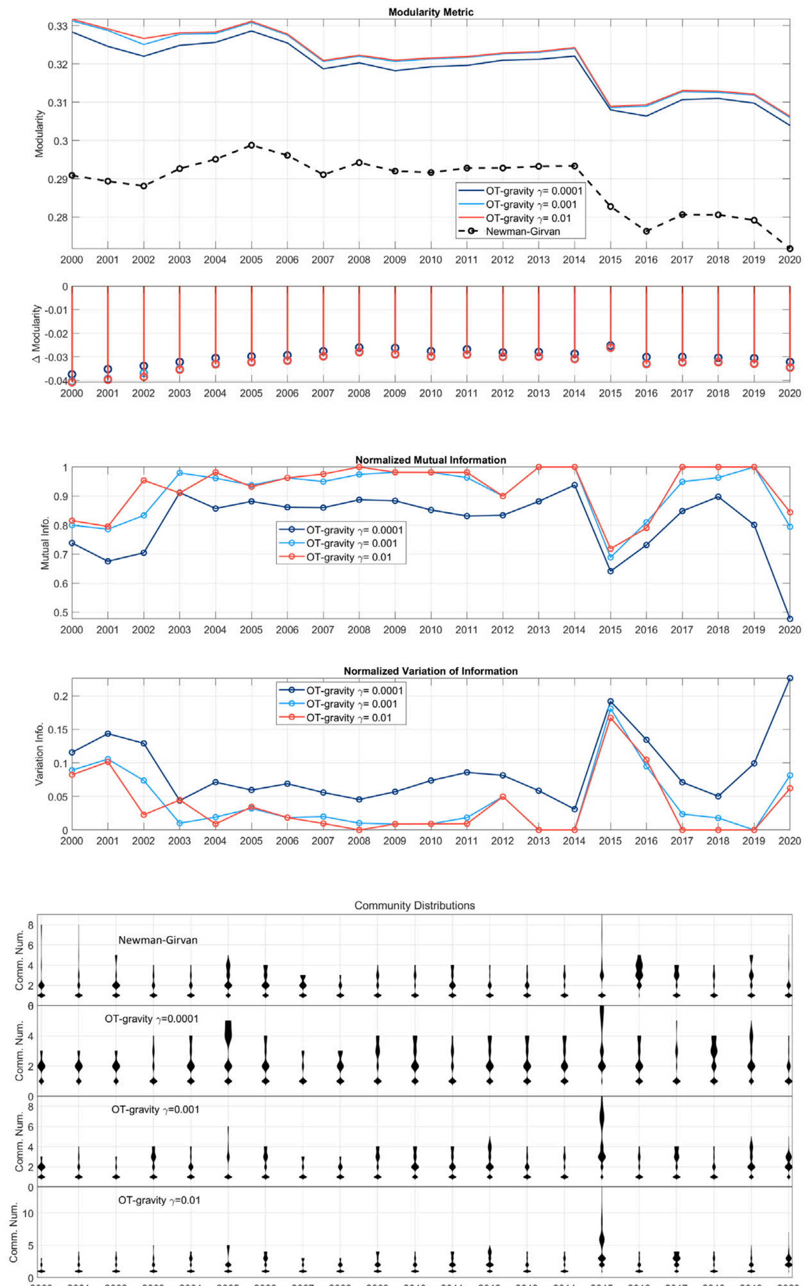

Fig. A.6. Community evaluation metrics for Poisson estimation. The figure reports the evolution of some community metrics obtained with the Poisson regression. In particular, the first two panels show the modularity and the change in the modularity values for the different models. Central panels show the normalized mutual and variation of information while lower panels summarize the change in the community distributions over time.

broad set of trade determinants) could provide a more flexible and data-adaptive alternative for generating expected trade flows, potentially leading to improved benchmarks for community detection.

CRediT authorship contribution statement

Rossana Mastrandrea: Writing – review & editing, Writing – original draft, Visualization, Software, Formal analysis, Data curation. **Paolo Pagnottoni:** Writing – review & editing, Writing – original draft, Validation, Supervision, Investigation. **Nicolò Pecora:** Writing – review & editing, Writing – original draft, Validation, Resources, Investigation, Data curation. **Alessandro Spelta:** Writing – review & editing, Writing – original draft, Software, Methodology, Investigation, Data curation, Conceptualization.

Declaration of competing interest

The authors declare that they have no known competing financial interests or personal relationships that could have appeared to influence the work reported in this paper.

Acknowledgments

NP and AS acknowledges the support by the Italian Ministry of University and Research (MUR) through the project “A geo-localized data framework for managing climate risks and designing policies to support sustainable investments” (No. 20229CWYXC) within the PRIN 2022 program, funded by the European Union – Next Generation EU.

RM acknowledges support from the project “THE - Tuscan Health Ecosystem” (CUP:D63C22000400001) and the PRIN 2022 project “The

Role of the Public and Private Sectors in Pharmaceutical Breakthrough Innovations (3PBI)" (CUP 2022S4EAS9). RM is member of GNAMPA (Gruppo Nazionale per l'Analisi Matematica, la Probabilità e le loro Applicazioni) at INdAM (Istituto Nazionale di Alta Matematica).

We thank two anonymous Reviewers for helpful and constructive comments.

Appendix. Results for alternative regression models

In this Appendix we report the results obtained by fitting alternative econometric models. In particular, we perform standard ordinary least squares (OLS) estimation applied to the log-linearized form of the gravity equation, replacing zeros with a small constant, and the Poisson regression model (see Figs. A.1–A.6).

References

Aldecoa, R., Marin, I., 2011. Deciphering network community structure by surprise. PLoS One 6 (9), e24195.
Almquist, Z.W., Butts, C.T., 2015. Predicting regional self-identification from spatial network models. Geogr. Anal. 47 (1), 50–72.
Anderson, J.E., 1979. A theoretical foundation for the gravity equation. Amer. Econom. Rev. 69 (1), 106–116.
Anderson, J.E., Larch, M., Yotov, Y.V., 2018. GEPPML: General equilibrium analysis with PPML. World Economy 41 (10), 2750–2782.
Anderson, J.E., Van Wincoop, E., 2003. Gravity with gravitas: A solution to the border puzzle. Amer. Econom. Rev. 93 (1), 170–192.
Baldwin, R., Taglioni, D., 2006. Gravity for dummies and dummies for gravity equations. Technical Report w12516, National Bureau of Economic Research.
Barigozzi, M., Fagiolo, G., Mangioni, G., 2011. Identifying the community structure of the international-trade multi-network. Physica A 390 (11), 2051–2066.
Beck, T., 2002. Financial development and international trade: Is there a link? J. Int. Econom. 57 (1), 107–131.
Bergstrand, J.H., 1985. The gravity equation in international trade: some microeconomic foundations and empirical evidence. Rev. Econom. Stat. 474–481.
Bertsekas, D.P., 1979. A distributed algorithm for the assignment problem. In: Lab. for Information and Decision Systems Working Paper. MIT.
Bhattacharya, K., Mukherjee, G., Saramäki, J., Kaski, K., Manna, S.S., 2008. The international trade network: weighted network analysis and modelling. J. Stat. Mech. Theory Exp. 2008 (02), P02002.
Bollen, J., Freeman, D., Teulings, R., 2020. Trade policy analysis with a gravity model. CPB Backgr. Doc. 17.
Brandes, U., Delling, D., Gaertler, M., Gorke, R., Hoefer, M., Nikoloski, Z., Wagner, D., 2007. On modularity clustering. IEEE Trans. Knowl. Data Eng. 20 (2), 172–188.
Breiman, L., 2017. Classification and Regression Trees. Routledge.
Brun, J.-F., Carrère, C., Guillaumont, P., De Melo, J., 2005. Has distance died? Evidence from a panel gravity model. World Bank Econom. Rev. 19 (1), 99–120.
Burger, M., Van Oort, F., Linders, G.-J., 2009. On the specification of the gravity model of trade: zeros, excess zeros and zero-inflated estimation. Spat. Econom. Anal. 4 (2), 167–190.
Butts, C.T., 2003. Network inference, error, and informant (in) accuracy: a Bayesian approach. Soc. Netw. 25 (2), 103–140.
Butts, C.T., 2012. Space and Structure: Methods and Models for Large-Scale Interpersonal Networks. Springer New York.
Butts, C.T., Acton, R.M., 2011. Spatial modeling of social networks. In: The Sage Handbook of GIS and Society Research. Thousand Oaks. SAGE Publications, CA, pp. 222–250.
Butts, C.T., Acton, R.M., Hipp, J.R., Nagle, N.N., 2012. Geographical variability and network structure. Soc. Netw. 34 (1), 82–100.
Chaney, T., 2008. Distorted gravity: heterogeneous firms, market structure, and the geography of international trade. Amer. Econom. Rev. 98 (4), 1707–1721.
Chaney, T., 2018. The gravity equation in international trade: An explanation. J. Political Economy 126 (1), 150–177.
Chen, M., Kuzmin, K., Szymanski, B.K., 2014. Community detection via maximization of modularity and its variants. IEEE Trans. Comput. Soc. Syst. 1 (1), 46–65.
Chen, Y., Lin, Z., Müller, H.-G., 2021. Wasserstein regression. J. Amer. Statist. Assoc. 1–14.
Cho, W., Lee, D., Kim, B.J., 2023. A multiresolution framework for the analysis of community structure in international trade networks. Sci. Rep. 13 (1), 5721.
Conley, T.G., Gonçalves, S., Kim, M.S., Perron, B., 2023. Bootstrap inference under cross-sectional dependence. Quant. Econom. 14 (2), 511–569.
Cristianini, N., Shawe-Taylor, J., 2000. An Introduction to Support Vector Machines and Other Kernel-Based Learning Methods. Cambridge University Press.
Cuturi, M., 2013. Sinkhorn distances: Lightspeed computation of optimal transport. Adv. Neural Inform. Process. Syst. 26.
Daraganova, G., Pattison, P., Koskinen, J., Mitchell, B., Bill, A., Watts, M., Baum, S., 2012. Networks and geography: Modelling community network structures as the outcome of both spatial and network processes. Soc. Netw. 34 (1), 6–17.
De Benedictis, L., Taglioni, D., 2011. The Gravity Model in International Trade. Springer.
De Benedictis, L., Tajoli, L., 2011. The world trade network. World Economy 34 (8), 1417–1454.
De Giuli, M.E., Spelta, A., 2023. Wasserstein barycenter regression for estimating the joint dynamics of renewable and fossil fuel energy indices. Comput. Manag. Sci. 20 (1), 1.
Duenas, M., Fagiolo, G., 2013. Modeling the international-trade network: a gravity approach. J. Econom. Interact. Coordinat. 8, 155–178.
Evenett, S.J., Keller, W., 2002. On theories explaining the success of the gravity equation. J. Political Econom. 110 (2), 281–316.
Expert, P., Evans, T.S., Blondel, V.D., Lambiotte, R., 2011. Uncovering space-independent communities in spatial networks. Proc. Natl. Acad. Sci. 108 (19), 7663–7668.
Fagiolo, G., 2010. The international-trade network: gravity equations and topological properties. J. Econom. Interact. Coordinat. 5, 1–25.
Fagiolo, G., Reyes, J., Schiavo, S., 2008. On the topological properties of the world trade web: A weighted network analysis. Physica A 387 (15), 3868–3873.
Fally, T., 2015. Structural gravity and fixed effects. J. Int. Econom. 97 (1), 76–85.
Fan, Y., Ren, S., Cai, H., Cui, X., 2014. The state's role and position in international trade: A complex network perspective. Econom. Model. 39, 71–81.
Fortunato, S., 2010. Community detection in graphs. Phys. Rep.- Rev. Sec. Phys. Lett. 486, 75–174.
Fortunato, S., Barthelemy, M., 2007. Resolution limit in community detection. Proc. Natl. Acad. Sci. 104, 36–41.
Fortunato, S., Hric, D., 2016. Community detection in networks: A user guide. Phys. Rep. 659, 1–44.
Fronczak, A., Fronczak, P., 2012. Statistical mechanics of the international trade network. Phys. Rev. E 85 (5), 056113.
García-Pérez, G., Boguñá, M., Allard, A., Serrano, M.Á., 2016. The hidden hyperbolic geometry of international trade: World Trade Atlas 1870–2013. Sci. Rep. 6 (1), 33441.
Garlaschelli, D., Di Matteo, T., Aste, T., Caldarelli, G., Loffredo, M.I., 2007. Interplay between topology and dynamics in the world trade web. Eur. Phys. J. B 57, 159–164.
Garlaschelli, D., Loffredo, M.I., 2004a. Fitness-dependent topological properties of the world trade web. Phys. Rev. Lett. 93 (18), 188701.
Garlaschelli, D., Loffredo, M.I., 2004b. Patterns of link reciprocity in directed networks. Phys. Rev. Lett. 93 (26), 268701.
Girvan, M., Newman, M.E., 2002. Community structure in social and biological networks. Proc. Natl. Acad. Sci. 99 (12), 7821–7826.
Good, B.H., De Montjoye, Y.-A., Clauset, A., 2010. Performance of modularity maximization in practical contexts. Phys. Rev. E 81 (4), 046106.
Hummels, D., 1999. Toward a geography of trade costs. Univ. Chic..
Jin, D., Yu, Z., Jiao, P., Pan, S., He, D., Wu, J., Philip, S.Y., Zhang, W., 2021. A survey of community detection approaches: From statistical modeling to deep learning. IEEE Trans. Knowl. Data Eng. 35 (2), 1149–1170.
Kali, R., Reyes, J., 2007. The architecture of globalization: a network approach to international economic integration. J. Int. Bus. Stud. 38, 595–620.
Kali, R., Reyes, J., 2010. Financial contagion on the international trade network. Econom. Inq. 48 (4), 1072–1101.
Klecka, W.R., 1980. Discriminant Analysis. Vol. 19, Sage.
Kuhn, H.W., 1955. The hungarian method for the assignment problem. Nav. Res. Logist. Q. 2 (1–2), 83–97.
Lancichinetti, A., Fortunato, S., 2011. Limits of modularity maximization in community detection. Phys. Rev. E— Stat. Nonlinear, Soft Matter Phys. 84 (6), 066122.
Larch, M., Wanner, J., Yotov, Y.V., Zylkin, T., 2019. Currency unions and trade: a PPML re-assessment with high-dimensional fixed effects. Oxf. Bull. Econom. Stat. 81 (3), 487–510.
Leamer, E.E., Levinsohn, J., 1995. International trade theory: the evidence. Handb. Int. Econom. 3, 1339–1394.
Leibovici, F., 2021. Financial development and international trade. J. Political Econom. 129 (12), 3405–3446.
Linders, G.-J., De Groot, H.L., 2006. Estimation of the gravity equation in the presence of zero flows. Tinbergen Institute Discussion Paper.
Luckstead, J., Devadoss, S., Zhao, X., 2024. Gravity trade model with firm heterogeneity and horizontal foreign direct investment. Amer. J. Agric. Econom. 106 (1), 206–225.
Malliaros, F.D., Vazirgiannis, M., 2013. Clustering and community detection in directed networks: A survey. Phys. Rep. 533 (4), 95–142.
Mastrandrea, R., Squartini, T., Fagiolo, G., Garlaschelli, D., 2014. Enhanced reconstruction of weighted networks from strengths and degrees. New J. Phys. 16 (4), 043022.
Newman, M.E., 2004. Detecting community structure in networks. Eur. Phys. J. B 38, 321–330.
Newman, M.E., 2006. Modularity and community structure in networks. Proc. Natl. Acad. Sci. 103 (23), 8577–8582.

Newman, M.E.J., Girvan, M., 2004. Finding and evaluating community structure in networks. Phys. Rev. E 69, 026113.
Overman, H.G., Redding, S., Venables, A.J., 2003. The economic geography of trade, production, and income: a survey of empirics. Handb. Int. Trade 350–387.
Pecora, N., Rovira Kaltwasser, P., Spelta, A., 2016. Discovering SIFIs in interbank communities. PLoS One 11 (12), e0167781.
Pele, O., Werman, M., 2009. Fast and robust earth mover's distances. In: 2009 IEEE 12th International Conference on Computer Vision. IEEE, pp. 460–467.
Petersen, A., Liu, X., Divani, A.A., 2021. Wasserstein F-tests and confidence bands for the fréchet regression of density response curves. Ann. Statist. 49 (1), 590–611.
Piccardi, C., Tajoli, L., 2012. Existence and significance of communities in the world trade web. Phys. Rev. E 85 (6), 066119.
Porter, M.A., Onnela, J.-P., Mucha, P.J., et al., 2009. Communities in networks. SSRN.
Preciado, P., Snijders, T.A., Burk, W.J., Stattin, H., Kerr, M., 2012. Does proximity matter? Distance dependence of adolescent friendships. Soc. Netw. 34 (1), 18–31.
Rosvall, M., Bergstrom, C.T., 2008. Maps of random walks on complex networks reveal community structure. Proc. Natl. Acad. Sci. 105 (4), 1118–1123.
Rubner, Y., Guibas, L.J., Tomasi, C., 1997. The earth mover's distance, multi-dimensional scaling, and color-based image retrieval. In: Proceedings of the ARPA Image Understanding Workshop. Vol. 661, p. 668.
Saracco, F., Di Clemente, R., Gabrielli, A., Squartini, T., 2016. Detecting early signs of the 2007–2008 crisis in the world trade. Sci. Rep. 6 (1), 30286.
Schiavo, S., Reyes, J., Fagiolo, G., 2010. International trade and financial integration: a weighted network analysis. Quant. Finance 10 (4), 389–399.
Serrano, M.A., Boguná, M., 2003. Topology of the world trade web. Phys. Rev. E 68 (1), 015101.
Serrano, M.Á., Boguñá, M., Vespignani, A., 2007. Patterns of dominant flows in the world trade web. J. Econom. Interact. Coordinat. 2 (2), 111–124.
Silva, J.S., Tenreyro, S., 2006. The log of gravity. Rev. Econom. Stat. 88 (4), 641–658.
Spelta, A., Pecora, N., 2024. Wasserstein barycenter for link prediction in temporal networks. J. R. Stat. Soc. Ser. A: Stat. Soc. 187 (1), 180–208.
Squartini, T., Garlaschelli, D., 2015. Stationarity, non-stationarity and early warning signals in economic networks. J. Complex Netw. 3 (1), 1–21.
Tajoli, L., Airoldi, F., Piccardi, C., 2021. The network of international trade in services. Appl. Netw. Sci. 6 (1), 1–25.
Villani, C., 2009. Optimal Transport: Old and New. Vol. 338, Springer.
Yang, J., McAuley, J., Leskovec, J., 2013. Community detection in networks with node attributes. In: 2013 IEEE 13th International Conference on Data Mining. IEEE, pp. 1151–1156.
Yotov, Y.V., 2024. The evolution of structural gravity: The workhorse model of trade. Contemp. Econom. Policy 42 (4), 578–603.
Yotov, Y.V., Piermartini, R., Larch, M., et al., 2016. An Advanced Guide to Trade Policy Analysis: The Structural Gravity Model. WTO iLibrary.
Zhu, Z., Cerina, F., Chessa, A., Caldarelli, G., Riccaboni, M., 2014. The rise of China in the international trade network: a community core detection approach. PLoS One 9 (8), e105496.